Published in final edited form as:
J Biomech Eng. 2008 December ; 130(6): 061019. doi:10.1115/1.2939273.

Field Variable Associations With Scratch Orientation-Dependence of UHMWPE Wear: A Finite Element Analysis

Matthew C. Paul[†,*,‡], **Liam P. Glennon**[†,*], **Thomas E. Baer**[†], and **Thomas D. Brown**[†,*]

† *Department of Orthopaedics and Rehabilitation, University of Iowa, Iowa City, IA*

* *Department of Biomedical Engineering, University of Iowa, Iowa City, IA*

‡ *Wright Medical Technology, Inc., Arlington, TN*

Abstract

Background—Scratches on the metal bearing surface of metal-on-polyethylene total joint replacements have been found to appreciably accelerate abrasive/adhesive wear of polyethylene, and constitute a source of the considerable variability of wear rate seen within clinical cohorts. Scratch orientation with respect to the local direction of relative surface sliding is presumably a factor affecting instantaneous debris liberation during articulation.

Method of Approach—A three-dimensional local finite element model was developed of orientation-specific polyethylene articulation with a scratched metal counterface, to explore continuum-level stress/strain parameters potentially correlating with the orientation dependence of scratch wear in a corresponding physical experiment.

Results—Computed maximum stress values exceeded the yield strength of ultra-high molecular weight polyethylene (UHMWPE) for all scratch orientations, but did not vary appreciably among scratch orientations. Two continuum-level parameters judged most consistent overall with the direction dependence of experimental wear were: (1) cumulative compressive total normal strain in the direction of loading, and (2) maximum instantaneous compressive total normal strain transverse to the sliding direction.

Conclusions—Such stress/strain metrics could be useful in global computational models of wear acceleration, as surrogates to incorporate anisotropy of local metal surface roughening.

Keywords

wear; wear surrogate; scratch wear; scratch orientation; finite element analysis; arthroplasty; THA; TKA; polyethylene; UHMWPE

INTRODUCTION

Roughening of the metal counterface is responsible for substantial increase of wear rate in metal-on-polyethylene total joint replacements [1–4]. This arguably is the cause of much of the variability in wear rates and wear directions seen among individual patients within study cohorts [5–7]. Retrieved femoral heads often show scratch damage (burnishing) involving substantial fractions of the head surface area. Determination of a consistent and direct relationship between conventional tribologic mean surface roughness parameters (R_a, R_p, etc.) and ensuing implant wear has proven elusive [8–10]. This has prompted several groups to study

Corresponding author: Thomas D. Brown, Ph.D., Orthopaedic Biomechanics Laboratory, 2181 Westlawn, University of Iowa Iowa City, IA 52242. (319) 335-7528, Fax: (319) 335-7530, Email: tom-brown@uiowa.edu.

scratch patterns, toward a more definitive determinant of wear acceleration propensity [1,9,11]. Scratches are widely regarded as resulting from 3rd body ingress into the bearing surface, the debris responsible being in forms such as bone mineral crystals, bone cement particles, radio-opacifier particles, porous coating particles, or metal frettings [8,9,12–14]. It has been argued that even some 3rd body particles that are (moderately) softer than the counterface are capable of causing scratching [14].

Scratch-induced wear of polyethylene (conventional or crosslinked) in total hip arthroplasty (THA) is due to local material failure. It seems reasonable that the direction of scratches on the metal counterface, relative to the direction of local sliding of the opposing polyethylene, would have an effect on the amount of wear produced during articulation. Past research involving scratch wear has presumed that the greatest wear occurs with scratches oriented perpendicular (90º) to the direction of motion [15–22]. Plausibly, however, more wear debris might well be liberated at a more acute attack angle, for example, from shearing-off of polyethylene by scratch lip asperities.

Recent developments in whole-joint computational wear simulation have proven helpful for understanding individual prosthesis design parameters [23], and for understanding the relative criticality of specific roughened regions in terms of accelerating wear [24]. To date, however, such models have not addressed scratch directionality. Such anisotropic influence might be implemented at the global analysis level using appropriate continuum surrogates, given formal mappings of scratch topography. Toward that end, a local computational model was developed to phenomenologically survey which stress/strain tensorial component(s), or which metric(s) involving several such components, might show orientation dependence resembling that observed experimentally. Such surrogate(s) could be useful to account for scratch-direction-dependent wear acceleration in global computational models incorporating anisotropic surface damage.

MATERIALS AND METHODS

The physical experiment to which the (below-described) finite element model was matched involved reciprocal motions of arrays of 550 parallel scratches, diamond-scribed at 150-μm intervals on lapped ($R_a < 100$ nm) 316L stainless steel plates. These scratches had nominal lip heights, lip widths and furrow widths of 1.3, 22 and 23 μm, respectively (Figure 1). The width of inter-scratch spacing and the dimensions of the individual scratches (which resemble typical large scratches found on retrievals [15]) were such as to produce a substantial volume of wear in a relatively short time. This severe degree of damage was not intended to directly replicate an *in situ* articular environment, but rather to generate sufficient wear to facilitate discrimination of the effect of scratch directionality.

Using a Scotch yoke pin-on-plate fixture installed on a biaxial load frame, the scratched counterface plate was driven reciprocally against a simple flat-ended cylindrical 25.4 mm diameter polyethylene pin[1] (Figure 2), while loaded axially by 1269 N (nominal stress = 2.5 MPa). Parametric tests were conducted, in which the plate was moved across the polyethylene pin at angles of 0, 2.5, 5, 10, 15, 20, 30, 45, 60, and 90º relative to the scratch orientation. This was done both for both conventional polyethylene (CPE, HSS Reference, 4150HP, Poly Hi Solidur, Ft. Wayne, IN [25]) and for highly crosslinked polyethylene (HXPE, DePuy Marathon®[2], Warsaw, IN). The contact surface was kept immersed in 100% fetal bovine serum (treated with 10 mM EDTA and 0.01% sodium azide to prevent microbial growth), with wear periodically assessed gravimetrically. Tests were run to 90,000 cycles at an average (sinusoidal) sliding speed of 72 mm/s, with steady-state behavior typically ensuing at about 60,000 cycles.

NIH-PA Author Manuscript

NIH-PA Author Manuscript

A three-dimensional local finite element model (Figures 2,3) of this experiment was developed, to explore continuum-level stress/strain parameters potentially correlating with the direction-dependent interaction observed experimentally. Scratch-angle-specific meshes were generated to replicate the orientations of scratch traverse in the physical wear experiment. A loaded scratch was driven under displacement control across the polyethylene surface (Figure 3), with stress/strain data being registered at fiducial elements on the surface throughout course of scratch approach, over-passage and recession.

Finite element geometries were defined and meshed using PATRAN (r3, MSC.Software Corporation, Santa Ana, CA). These were input to the ABAQUS solver (v 6.4-2, ABAQUS, Inc., Pawtucket, RI), and were post-processed using ABAQUS/Viewer. Additional post-processing was performed using scripts custom-written in MATLAB 6.5.1 (The Mathworks, Inc., Natick, MA).

Although a suitably refined local finite element model for the entire testing interface would have been intractable, the physical system's periodicity allowed isolating a single scratch. This assumed, effectively, that the same local instantaneous stress-strain history would recur over and over at a given point on the polyethylene surface, due to large numbers of over-passages of identical scratches. A provisional assumption was made (subsequently verified computationally) that the inter-scratch-lip distance, scratch lip height, polyethylene material properties, and loading were such that contact occurred only on scratch lips, rather than also on the (flat) inter-scratch regions of the metal surface. Accordingly, the corresponding load per unit scratch lip length (185 N/m for the 1269 N loads used experimentally) was employed in the computational model. Since the polyethylene pin remained entirely within the scratched region of the plate, the total length of scratch lip "line contact" (6.8 m) remained constant throughout the duty cycle. A rectangular polyethylene solid of finite size and appropriate aspect ratio [26] was generated for each specific scratch orientation.

Topographic data from a representative scratch lip profile were captured using a laser scanning microscope (0.01 μm depth accuracy, 0.3 μm sampling resolution), and directly transferred to the finite element model (Figure 1). Both the polyethylene surface and inter-scratch areas of the metal plate were modeled as flat.

Constitutively, UHMWPE was modeled using a fourth-order relationship for tangent modulus E as a function of von Mises stress, as reported by Cripton [27]. An h-convergence series run for a nominally corresponding Hertzian contact problem [26] established that 0.3334 μm was an appropriate dimension for the polyethylene elements. A rigid-on-deformable local contact condition was invoked, with a Coulombic friction coefficient of 0.038 [28]. The analysis was quasi-static and modeled nonlinear contact geometry. Boundary conditions specified for the respective faces of the polyethylene block were configured so as to have the block approximate an infinite half-space [26].

The provisionally assumed simplification of the counterface topography to a single scratch lip was justified using a 2-D plane strain finite element simulation of sliding contact [26], executed for nonlinear UHMWPE, under the full prescribed service load of 185 N/m. Under these conditions, stress field "disturbances" from neighboring scratches were effectively isolated from each other, as indeed even were those from the two scratch lips on opposing sides of a given scratch furrow. A reference node representing the rigid Bezier surface of the scratch lip was utilized to prescribe the kinematics of the scratch lip.

A metric was formulated to reflect cumulative mechanical stimulus to the polyethylene during an event of scratch approach, over-passage, and recession. Full tensorial stress and strain data were output for five fiducial elements located centrally on the polyethylene, at serial instants (typically, 50) throughout the slide event. The overall putative stimulus Φ delivered to a given site on the polyethylene during a scratch encounter was indexed as follows. Consider a plausibly physically consequential instantaneous surrogate wear parameter φ. For example, φ might be an individual component of stress or an individual component of strain, or a function derived from some combination thereof (e.g., strain energy density). For a quasi-static sliding event, the cumulative stimulus Φ (Equation 1) can be characterized in terms of the history integral of the instantaneous value of the candidate stimulus parameter, i.e.,

$$\Phi=\int_{t=-\infty}^{t=\infty} \varphi \cdot dt \tag{1}$$

In the context of finite element analysis, where solutions are reported only at discrete times, and where (for tractability) the analysis is restricted only to the immediate “time neighborhood” of appreciable stress disturbance due to scratch encounter, the corresponding discretized expression (Equation (2)) is

$$\Phi=\sum_{i=i_0}^{i=i_{\max}} \varphi_i \Delta t_i \tag{2}$$

Here, i_0 is the first finite element solution increment for which supra-background stress ensues with oncoming scratch approach, i_{max} is the last solution increment for which supra-background stress persists as the scratch recedes after over-passage, and Δt_i is the time increment between successive FEA solution reports.

The dimensional units of the kernel (φ) and the integrand (Φ) varied, according to the specific composition of the candidate mechanical stimulus. To facilitate commonality of subsequent correlation comparisons of potential surrogates with experimentally observed volumetric wear rates (units of mm^3*/million cycles per* mm^2 of platen area, *A*, engaged), a dimensional compensation term γ was included in the surrogate computational volumetric wear ($\hat{V}$) prediction expression, Equation (3).

$$\widehat{V}=A * \Phi * \gamma \tag{3}$$

For example, if the candidate kernel parameter φ was compressive normal stress σ_{22}, the units of *A* *Φ would be mm^2 (for *A*)* $\frac{N \cdot \text{sec}}{mm^2}$ (for Φ), i.e. *N* •sec, in which case γ would need to take units of $\frac{mm^3}{million \cdot cycles \cdot N \cdot \text{sec}}$. Thus, the units for each term in Equation (3) would be $\frac{mm^3}{million \cdot cycles}=mm^2 * \frac{N \cdot \text{sec}}{mm^2} * \frac{mm^3}{million \cdot cycles \cdot N \cdot \text{sec}}$.

Four separate registry treatments were considered to implement the Φ summation. The first of these involved summing all incremental kernel values, without segregating by algebraic sense; that is, negative values were combined with positive values, thus admitting the possibility of partial cancellation. In the second treatment, absolute values of each incremental φ were summed. The third and fourth treatments involved summing only the positive and only the negative φ values, respectively. Additionally, four non-summation-based metrics of mechanical stimulus were considered: the maximum peak-to-valley excursion for each kernel parameter φ, and that kernel parameter’s algebraic maximum, algebraic minimum, and absolute maximum throughout the scratch passage event.

Wear correlations with plastic strains areas were also considered, prompted by the localized scratch finite element model reported by McNie *et al.* [29]. For each scratch orientation, a predetermined set of centrally-located surface/subsurface fiducial elements were interrogated for plastic strains occurring above specific thresholds. The total cross-sectional area (in the plane of the axes of loading and motion) was summed for those elements experiencing supra-threshold strains at any instant during the scratch encounter. The maximum instantaneous area of plastic strain above these specific thresholds was registered, as were the areas for principal plastic strain and maximum plastic shear strain. Again, plastic strain area results were segregated by maximum positive and negative values of strain, respectively, maximum absolute magnitudes of strain, and by residual plastic strain. These plastic strain areas were tabulated for 20 different plastic strain thresholds, spanning two orders of magnitude (0, 0.0005, 0.001–0.01 by increments of 0.001, and 0.01–0.09 by increments of 0.01). Additionally, the scratch angle dependence of the product of maximum instantaneous area of plastic strain times magnitude of plastic strain was investigated, for all four of the above-segregated areas and all 20 plastic strain thresholds. In total, 1,027 different stimulus variants were considered as possible surrogate metrics of wear, both for conventional and for highly crosslinked polyethylene (2,054 comparisons overall).

For both polyethylene variants, correspondence of the candidate metrics with the experimentally observed scratch direction-dependence of wear was evaluated both by objective measures of goodness-of-fit, and visually for specific qualitative criteria. All candidate metrics were formally ranked according to the average of three goodness-of-fit measures. The first of these measures was the cross-correlation coefficient *r*, defined [30] as follows:

$$r=\frac{\sum_{i}^{n_\theta}(\Phi(i)-m_\Phi)(\widehat{V}(i)-m_{\widehat{V}})}{\sqrt{\sum_{i}^{n_\theta}(\Phi(i)-m_\Phi)^2}\sqrt{\sum_{i}^{n_\theta}(\widehat{V}(i)-m_{\widehat{V}})^2}} \quad (4)$$

Here, Φ and $\hat{V}$ represent values of the surrogate metric and the experimental wear for a set of n_θ scratch angles, with $m\Phi$ and m_V denoting the respective means. The second goodness-of-fit measure was the area fraction Â shared by two respective wear-vs-direction curves, after normalization to ensure equal areas. The third measure of fit was an R^2 correlative statistic emerging from a random-fixed effects regression model. Briefly (details in Appendix A), analysis of variance (ANOVA) was performed both including and not including the computational dataset as a predictor of the experimental dataset. The improvement in variance achieved by adding the computational dataset as a predictor yielded an R^2 statistic for that computational dataset. For visual assessments, plots of each φ parameter were reviewed manually throughout the individual scratch passage event, as were (normalized) plots of the corresponding Φ values versus angle-dependent experimental wear.

RESULTS

Experimentally, for conventional UHMWPE, a scratch oriented at 15º with respect to the sliding direction produced the greatest wear. The direction of greatest wear for crosslinked UHMWPE was 5º. In the finite element model, maximum stress values did not vary appreciably with scratch orientation. Rather, UHMWPE stresses achieved similarly supra-yield magnitudes for all scratch orientations. Peak normal stresses and principal stresses typically approached 60 MPa during scratch over-passage, while peak shear stresses were typically on the order of 10 MPa.

Two continuum wear surrogates were judged to most reasonably resemble the scratch lip direction-dependence observed experimentally. These two best-performing surrogates were (1) the cumulative compressive total normal strain in the direction of loading, and (2) the maximum instantaneous compressive total normal strain in the direction transverse to sliding (Figure 4). "Total strain" in this context denotes the sum of elastic plus plastic logarithmic strain.

A truncated list of candidate surrogates demonstrating the best quality of fit to scratch-direction-dependent experimental wear is presented in Table 1. Overall, the various surrogates computed in the finite element simulation did not show an ability to better fit the angle-dependence of one polyethylene material variant as opposed to the other. The entire quality-of-fit distribution is presented in Figure 5. Illustrative angle-dependencies of fits of candidate metrics are displayed in Figure 6, demonstrating the spectrum of predictive capability. The relative performance of these particular parameters (with respect to the complete set of available candidates) can be appreciated from Figure 5.

Once the complete list of candidate mechanical stimulus parameters was ranked according to quality-of-fit Q, the highest-ranking candidates (those with $Q \geq 0.5$) were further screened visually, to ensure that they met four qualitative criteria. First, because desirable surrogate candidates needed to have a direction-dependent relationship that tended toward a single maximum, candidates presenting multiple discrete maxima of similar magnitude were eliminated from consideration. Similarly, candidates showing a relatively uniform distribution were excluded, as were those that had a global maximum at a scratch angle inconsistent with the experimental relationship. Fourth, since both positive-valued and negative-valued variants were evaluated for most potential surrogates, it seemed reasonable not to place credence in a given candidate (*e.g.*, positive stress in the 2-direction) if its complement (negative stress in the 2-direction) was of far greater magnitude. Therefore, candidate surrogates involving normal stress were eliminated if their complement (reflecting physically distinct behavior in tension versus compression) was two or more orders of magnitude greater. Shear stress/strain components were eliminated if their complements were even nominally greater, since shear is physically similar for positive and negative values. Distribution choppiness (Fig 6a), per se, was not a basis for exclusion, provided that the Q value was high and that none of the above four exclusion criteria were applicable.

Two surrogates emerged as being overall most appropriate. These were (1) cumulative total (elastic + plastic) compressive normal strain in the direction of loading, and (2) maximum instantaneous total compressive normal strain transverse to the sliding direction. Secondary parametric influences (e.g., leading lip versus trailing lip passage, repeated lip passage residual strains) and variants of data normalization and interpolation are reported in detail elsewhere [26].

DISCUSSION

A reciprocal, unidirectional duty cycle was adopted experimentally in the interest of preserving consistent orientation between scratch direction and counterface motion, thereby allowing isolation of the specific effect - scratch directionality - under study. For wear of UHMWPE against polished counterfaces, it is well recognized that such a duty cycle fails to incorporate the crossing-path motions responsible for shearing off striations of polyethylene produced by asperity adhesion/abrasion, and thus tends to underestimate the wear occurring in the actual (*in vivo*) service environment [31,32]. In the present experimental embodiment, however, besides achieving the desired effect of isolating the variable of primary interest (scratch directionality), there is a potent (indeed, arguably dominant) crossing-path effect, owing to scratch obliquity.

Computationally, the vast majority of the candidate mechanical parameters that were considered as potential wear surrogates turned out to correlate unremarkably (*i.e.*, 1,984 of the 2,054 considered had $Q < 0.5$), or indeed even poorly (1,063 had $Q < 0.3$) with the experimentally observed scratch direction-dependence of polyethylene wear (Figure 6). The dominant shortcoming in that regard arose from failure to replicate the pronounced wear rate maximum consistently observed experimentally for scratches oriented at low angles (5–15°) relative to the sliding direction. The local FEA model did not incorporate a formal material failure criterion to directly model abrasive/adhesive wear, but many of the potential wear surrogates considered were parameters that are strongly associated with continuum-level material failure processes (*e.g.*, first principal stress with tensile failure, von Mises stress with shear failure). Thus, one might reasonably infer that, had the local FEA model formally implemented a material failure mode, the scratch angle-dependence of such a failure process (*e.g.*, tensile failure) would have been very highly correlated with the scratch angle-dependence of the failure-associated surrogate measure (*i.e.*, first principal stress).

Given the observed insensitivity of the local stress and strain fields to scratch angle, one would not expect these simple metrics to be good predictors of angle-dependent wear rate. However, for metrics which implicitly incorporate a kinematic effect (e.g., stress or strain components transverse to the sliding direction), or those which explicitly incorporate a cumulative stimulus during scratch overpassage, the opportunities for correlation with physical wear mechanisms would seemingly be better. Although none of the individual surrogate mechanical parameters that were evaluated showed highly precise ($Q > 0.9$) or strong ($Q > 0.7$) replication of the experimentally observed relationship between scratch angle and wear rate, a small subset of them showed modest correlation (70 had $Q > 0.5$). Such surrogates therefore might plausibly be useful for phenomenological prediction of wear in FEA models of local asperities, and/or for making adjustments to global-level FEA wear predictions to possibly account for anisotropic roughening effects. Also, given these best-correlating parameters' associations with specific physical failure mechanisms, one might also reasonably infer the failure mechanism(s) associated with polyethylene wear rate acceleration in the presence of 3rd body-induced scratch damage of a metal counterface. In that regard, a "slicing" paradigm suggests itself quite compellingly, rather than the sort of a "plowing" mechanism intuitively associated with scratches oriented nearly perpendicular to the direction of relative surface motion.

Obviously, the stress distributions computed in the present local finite element model were predicated on the numbers, spacing, and lip height of scratches being such that the global contact load was supported entirely by "line contact" with scratch lips, rather than being supported substantially by unscratched surface regions. While this local FEA model was a realistic replication of the corresponding physical testing set-up, the latter had been deliberately designed to generate very large amounts of debris in short periods of time, in order to accentuate possible directional differences. The particular scratch profile utilized experimentally and computationally was representative of typical *in vivo* 3rd body damage, but the numbers/spacing of such scratches in the model corresponded to a situation far more abusive than would conceivably be tolerable *in vivo*. (As a point of reference, the absolute wear factor for the present 15° scratch angle experiments for conventional polyethylene averaged 5×10^{-6} mm^3/N-m, whereas typical wear factors for borderline-wear-problematic THA implants are on the order of $1.2–1.9 \times 10^{-6}$ mm^3/N-m [39,108].) Nevertheless, even though the great majority of load in clinical THA constructs is presumably supported by polished/ undamaged surface regions rather than by scratch lips, the present data arguably isolate the direction-dependence of wear rate acceleration due to whatever population of scratches happens to be physically present.

The maximum instantaneous area of plastic strain during scratch engagement was found to correlate fairly well with the experimental scratch-direction-dependence of wear, supporting the results of McNie *et al*.'s 2-D FEA work on scratch asperity damage to UHMWPE [15,29]. The results of the present study are also consistent with that group's observation that the area (or volume, in the case of the present 3-D formulation) of polyethylene undergoing plastic

NIH-PA Author Manuscript

NIH-PA Author Manuscript

strain may more reliably relate to wear volume than does the magnitude of maximum plastic strain *per se*.

High surface and subsurface plastic strains have been associated with the initiation of both surface ripples [33] and with fatigue micro-cracks on or below the surface [29]. The migration of such micro-cracks to the surface is believed to promote formation of polyethylene debris, potentially encouraging liberation of fibers or ridges tens of microns in length [34]. In the present study, such large fibers were ubiquitous in particle populations harvested from the lubricant (Figure 7) when a scratched counterface was involved. As a negative control, an otherwise similar non-roughened metal plate (R_a< 100 nm) reciprocating against polyethylene produced particles of submicron or micron size (Figure 7), resembling the predominant volumetric fraction of particles observed to surround total joints *in vivo*.

In summary, a finite element model was used to investigate the sliding articulation of polyethylene with parametrically-oriented scratch lips, surveying field variable histories in an attempt to identify continuum parameters empirically associated with corresponding experimentally-determined wear dependence. All candidate parameters were graphically reviewed manually, and were formally ranked statistically. The best correlating of these surrogates - two variants of compressive total strain - potentially provide a basis by which to account for anisotropic scratch damage in global FEA models of accelerated wear due to articulation against roughened femoral heads.

Acknowledgements

This research was supported by grants from the NIH (AR46601, AR47653). Technical assistance was provided by Dr. N. M. Grosland, Dr. S. L. Hillis, Mr. W. D. Lack, Dr. D. R. Pedersen, and Mr. K. J. Stewart.

References

1. Cooper JR, Dowson D, Fisher J. Macroscopic and microscopic wear mechanisms in ultra-high molecular weight polyethylene. Wear 1993;162–64:378, 384.(Proceedings of the 9th International Conference on Wear of Materials, Apr 13–16 1993)
2. Wang A, Polineni VK, Stark C, Dumbleton JH. Effect of femoral head surface roughness on the wear of ultrahigh molecular weight polyethylene acetabular cups. Journal of Arthroplasty 1998;13:615, 20. [PubMed: 9741435]
3. McKellop H, Clarke IC, Markolf KL, Amstutz HC. Wear characteristics of UHMW polyethylene: a method for accurately measuring extremely low wear rates. Journal of Biomedical Materials Research 1978;12:895, 927. [PubMed: 739020]
4. Muratoglu OK, Burroughs BR, Christensen SD, Lozynsky A, Harris WH. In vitro knee simulator wear of highly crosslinked tibias articulating against explanted rough femoral components. Trans 50th Orth Res Soc 2004:0297.
5. Brown TD, Stewart KJ, Nieman JC, Pedersen DR, Callaghan JJ. Local head roughening as a factor contributing to variability of total hip wear: a finite element analysis. Journal of Biomechanical Engineering 2002;124:691, 8. [PubMed: 12596637]
6. Schmalzried TP, Dorey F, McClung C, Scott D. The contribution of wear mechanism(s) to variability in wear rates. Trans 45th Orth Res Soc 1999:0287.
7. Goldsmith AA, Dowson D, Wroblewski BM, Siney PD, Fleming PA, Lane JM. The effect of activity levels of total hip arthroplasty patients on socket penetration. J Arthroplasty 2001;16:620–7. [PubMed: 11503122]
8. Elfick AP, Hall RM, Pinder IM, Unsworth A. The influence of femoral head surface roughness on the wear of ultrahigh molecular weight polyethylene sockets in cementless total hip replacement. Journal of Biomedical Materials Research 1999;48:712, 8. [PubMed: 10490687]
9. Sychterz CJ, Engh CA Jr, Swope SW, McNulty DE, Engh CA. Analysis of prosthetic femoral heads retrieved at autopsy. Clin Orthop 1999;358:223–34. [PubMed: 9973995]

10. Elfick APD, Hall RM, Pinder IM, Unsworth A. The influence of femoral head surface roughness on the wear of ultrahigh molecular weight polyethylene sockets in cementless total hip replacement. J Biomed Mater Res 1999;48:712–718. [PubMed: 10490687]
11. Jasty M, Bragdon CR, Lee K, Hanson A, Harris WH. Surface damage to cobalt-chrome femoral head prostheses. Journal of Bone & Joint Surgery - British Volume 1994;76:73, 7. [PubMed: 8300686]
12. McKellop HA, Campbell P, Park SH, Schmalzried TP, Grigoris P, Amstutz HC, Sarmiento A. The origin of submicron polyethylene wear debris in total hip arthroplasty. Clinical Orthopaedics & Related Research 1995;311:3–20. [PubMed: 7634588]
13. Atkinson JR, Dowson D, Isaac GH, Wroblewski BM. Laboratory wear tests and clinical observations of the penetration of femoral heads into acetabular cups in total replacement hip joints: II. A microscopical study of the surfaces of Charnley polyethylene acetabular sockets. Wear 1985;104:225–244.
14. Mirghany M, Jin ZM. Prediction of scratch resistance of cobalt chromium alloy bearing surface, articulating against ultra-high molecular weight polyethylene, due to third-body wear particles. Proceedings of the Institution of Mechanical Engineers. Part H - Journal of Engineering in Medicine 2004;218:41, 50.
15. McNie CM, Barton DC, Ingham E, Tipper JL, Fisher J, Stone MH. Prediction of polyethylene wear rate and debris morphology produced by microscopic asperities on femoral heads. Journal of Materials Science: Materials in Medicine 2000;11:163–174. [PubMed: 15348045]
16. Endo MM, Barbour PS, Barton DC, Fisher J, Tipper JL, Ingham E, Stone MH. Comparative wear and wear debris under three different counterface conditions of crosslinked and non-crosslinked ultra high molecular weight polyethylene. Bio-Medical Materials & Engineering 2001;11:23–35. [PubMed: 11281576]
17. Minakawa H, Stone MH, Wroblewski BM, Lancaster JG, Ingham E, Fisher J. Quantification of third-body damage and its effect on UHMWPE wear with different types of femoral head. J Bone Joint Surg Br 1998;80:894–9. [PubMed: 9768905]
18. Fisher J, Firkins P, Reeves EA, Hailey JL, Isaac GH. The influence of scratches to metallic counterfaces on the wear of ultra-high molecular weight polyethylene. Proc Inst Mech Eng [H] 1995;209:263–4.
19. Dowson D. The role of counterface imperfections in the wear of polyethylene. Wear 1987;119:277–293.
20. Dharmastiti R, Barton DC, Fisher J, Edidin A, Kurtz S. The wear of orie nted UHMWPE under isotropically rough and scratched counterface test conditions. Bio-Medical Materials & Engineering 2001;11:241, 56. [PubMed: 11564907]
21. Kamali A, Farrar R, Stone MH, Fisher J. The effects of scratched femoral components on UHMWPE wear in rotating platform mobile bearing TKR. Trans 7th World Congress Biomaterials. 2004
22. Turell M, Wang A, Bellare A. Quantification of the effect of cross-path motion on the wear rate of ultra high molecular weight polyethylene. Wear 2003;255:1034–1039.
23. Maxian TA, Brown TD, Pedersen DR, Callaghan JJ. The Frank Stinchfield Award. 3-Dimensional sliding/contact computational simulation of total hip wear. Clin Orthop Relat Res 1996 Dec;(333): 41–50. [PubMed: 8981881]
24. Lundberg HJ, Stewart KJ, Callaghan JJ, Brown TD. Kinetically-critical sites of femoral head roughening for wear rate acceleration in total hip arthroplasty. Clin Orthop 2005;(430):89, 93. [PubMed: 15662308]
25. Bennet AP, Wright TM, Li S. Global reference UHMWPE: characterization and comparison to conventional UHMWPE. Trans 42nd Orth Res Soc 1996;21:472.
26. Paul, MC. Localized finite element analysis of orientation-specific scratch traverse across UHMWPE. Department of Biomedical Engineering, University of Iowa; 2004. M. S. Thesis
27. Cripton, PA. Compressive characterization of ultra-high molecular weight polyethylene with applications to contact stress analysis of total knee replacements. Queen's University at Kingston; 1993. M. S. Thesis
28. Scifert CF, Brown TD, Pedersen DR, Callaghan JJ. A finite element analysis of factors influencing total hip dislocation. Clin Orthop 1998 Oct;(355):152–62. [PubMed: 9917600]

29. McNie C, Barton DC, Stone MH, Fisher J. Prediction of plastic strains in ultra-high molecular weight polyethylene due to microscopic asperity interactions during sliding wear. Proceedings of the Institution of Mechanical Engineers. Part H - Journal of Engineering in Medicine 1998;212:49, 56.

30. Image Processing Toolbox User's Guide. Two–dimensional correlation coefficient between two matrices (Function reference corr2). 2004. The Mathworks, Inc., Natick, MA.

31. Bragdon CR, O'Connor DO, Lowenstein JD, Jasty M, Biggs SA, Harris WH. A new pin-on-disk wear testing method for simulating wear of polyethylene on cobalt-chrome alloy in total hip arthroplasty. J Arthroplasty 2001 Aug;16:658–65. [PubMed: 11503127]

32. Elfick AP, Hall RM, Pinder IM, Unsworth A. Wear in retrieved acetabular components: effect of femoral head radius and patient parameters. J Arthroplasty 1998 Apr;13(3):291–5. [PubMed: 9590640]

33. Wang A, Stark C, Dumbleton JH. Mechanistic and morphological origins of ultra-high molecular weight polyethylene wear debris in total joint replacement prostheses.[comment]. Proceedings of the Institution of Mechanical Engineers. Part H - Journal of Engineering in Medicine 1996;210:141, 55.

34. Wang A, Sun DC, Stark C, Dumbleton JH. Wear mechanisms of UHMWPE in total joint replacements. Wear 1995;181–183:241, 249.(Proceedings of the 10th International Conference on Wear of Materials, Apr 9–13 1995)

Appendix A

Random/Fixed-Effects Statistical Regression Model **M1** mean model with random subject effects:

$$y_{ij}=\beta_0+s_j+\varepsilon_{ij}$$

y_{ij} is the outcome for the

jth subject (scratched plate) $j = 1, 2, ..., n$,

ith angle $i = 1, 2, ..., t$

- $n = 3$ subjects/plates, $t = 10$ angles
- $N = nt = 3 \cdot 10 = 30$ total outcomes
- s_j (the subject effects) are normally distributed with mean 0 and variance σ^2
- ε_{ij} (individual observation errors) are normally distributed with mean 0 and variance σ^2

ANOVA table:

SOURCE	SS	df
subject	SS(subj) $t\sum_{j=1}^{n}(\bar{y}_{.j}-\bar{y}_{..})^2$	$n-1$
error(residual)	SS(error) $\sum_{i=1}^{t}\sum_{j=1}^{n}(y_{ij}-\bar{y}_{.j})^2$	$N-n-1$

SS(subj) – sum of squares due to subjects

SS(error) – sum of squares due to error (or residual)

Subscript $y.j$ denotes the average of all angles i, for subject j

Subscript $y..$ denotes the average of all subjects across all the angles

From these compute:

$$\text{MS(subj)}=\text{SS(subj)}/(n-1) \text{ and}$$

$$\text{MS(error)}=\text{SS(error)}/[N-n].$$

The variance estimates are the following:

$$\text{error variance}=\text{MS(error)}$$

$$\text{subject variance}=[\text{MS(subj)}-\text{MS(error)}]/n.$$

Note: if subject variance is negative, then it is set equal to 0.

M2 model with predictor and fixed subject effects:

$$y_{ij}=\beta_0+\beta_1 x_{ij}+s_j+\varepsilon_{ij}$$

where y_{ij}, s_j, and ε_{ij} are the same as before, and

x_{ij} is the predicted value for the outcome y_{ij} obtained from the candidate surrogate.

- Note that $x_{ij} = x_i$ (same prediction for each subject)
- Same assumptions on subject and error terms as in **M1**.

Slope and intercept estimates $\hat{\beta}_1$ and $\hat{\beta}_2$, using standard formulas for simple linear regression, are:

$$\widehat{\beta}_1=\frac{SS_{xy}}{SS_{xx}}=\frac{\sum_{i=1}^{t}\sum_{j=1}^{n}(x_{ij}-\overline{x})(y_{ij}-\overline{y})}{\sum_{i=1}^{t}\sum_{j=1}^{n}(x_{ij}-\overline{x})^2}=\frac{\sum_{i=1}^{t}\sum_{j=1}^{n}x_{ij}y_{ij}-N\overline{xy}}{\sum_{i=1}^{t}\sum_{j=1}^{n}x_{ij}^2-N\overline{x}^2} \quad \text{and} \quad \widehat{\beta}_0=\overline{y}-\widehat{\beta}_1\overline{x}$$

Alternatively, if applying MATLAB software, one can also use the matrix formula

$\underset{\sim}{\widehat{\beta}}=(X'X)^{-1}X\underset{\sim}{Y}$ where *X* contains a column vector of ones and a column vector with the *x* values (repeated three times end-to-end), *X'* denotes the transpose of *X*, and $\underset{\sim}{Y}$ is the outcome column vector of all three random subjects y_{i1}, y_{i2}, and y_{i3}, listed end-to-end.

Then $\underset{\sim}{\widehat{\beta}}=\begin{bmatrix}\widehat{\beta}_0\\ \widehat{\beta}_1\end{bmatrix}$

The predicted value, $\hat{y}_{ij}$, for each angle on each plate, using fixed subject effects, is:

$$\widehat{y}_{ij}=\widehat{\beta}_0+\widehat{\beta}_1 x_{ij}+\widehat{s}_j \quad (\text{where } x_{ij}=x_i)$$

- we treat subjects as fixed
- $s_j = \bar{y}_{.j} - \bar{y}_{..}$ is the estimate for subject effect, treating subjects as fixed.

ANOVA table:

SOURCE	SS	df
subject	SS(subj) $t\sum_{j=1}^{n}(y_{.j}-y_{..})^2$	$n-1$
error(residual)	SS(error) $\sum_{i=1}^{t}\sum_{j=1}^{n}(y_{ij}-\hat{y}_{ij})^2$	$N-n$

Then, with

$$\text{MS(subj)}=\text{SS(subj)}/(\text{n}-1)\ \text{ and MS(error)}=\text{SS(error)}/[N-n-1],$$

the variance estimates are again:

$$\text{error variance}=\text{MS(error) and subject variance}=[\text{MS(subj)}-\text{MS(error)}]/n.$$

$$\begin{aligned}&\text{Then } \mathbf{R-squared} \text{ is } (\text{var1}-\text{Var2})/\text{Var1}=\\&[(\mathbf{M1}\text{ subject variance}+\mathbf{M1}\text{ residual variance})\\&-(\mathbf{M2}\text{ subject variance}+\mathbf{M2}\text{ residual variance})]\\&/(\mathbf{M1}\text{ subject variance}+\mathbf{M1}\text{ residual variance})\end{aligned}$$

NIH-PA Author Manuscript
NIH-PA Author Manuscript

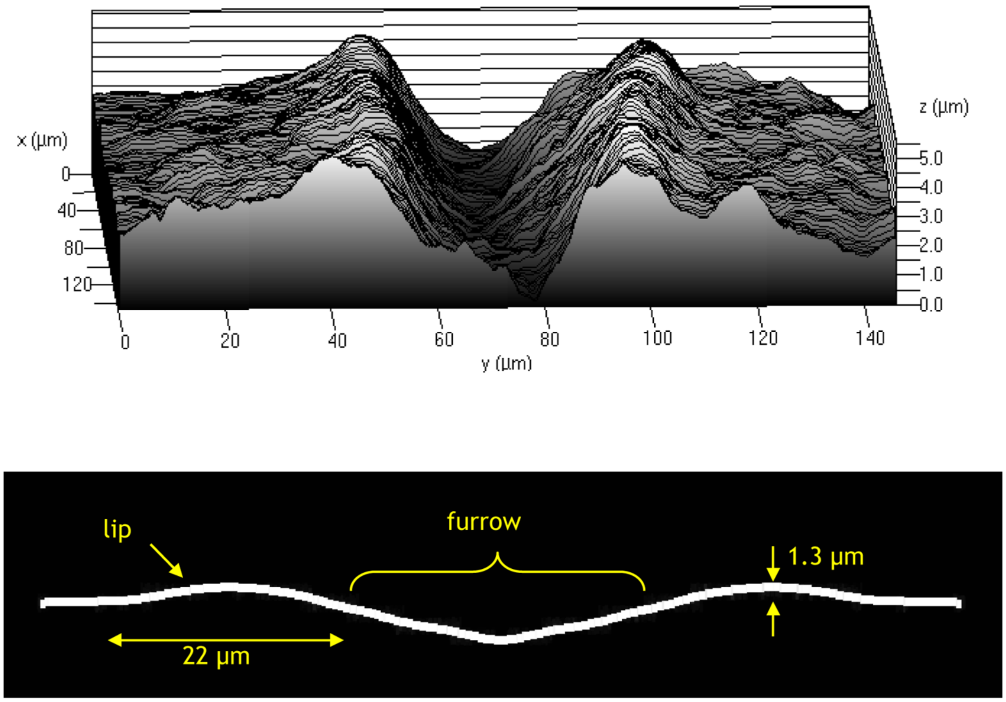

Figure 1.

(Top) Laser scanning microscopy image of custom scratch profile created on 316L stainless steel. (Note the scale differences, which accentuate the scratch for visual emphasis.) (Bottom) Scratch profile (cross-section) employed as the counterface surface in the FE model.

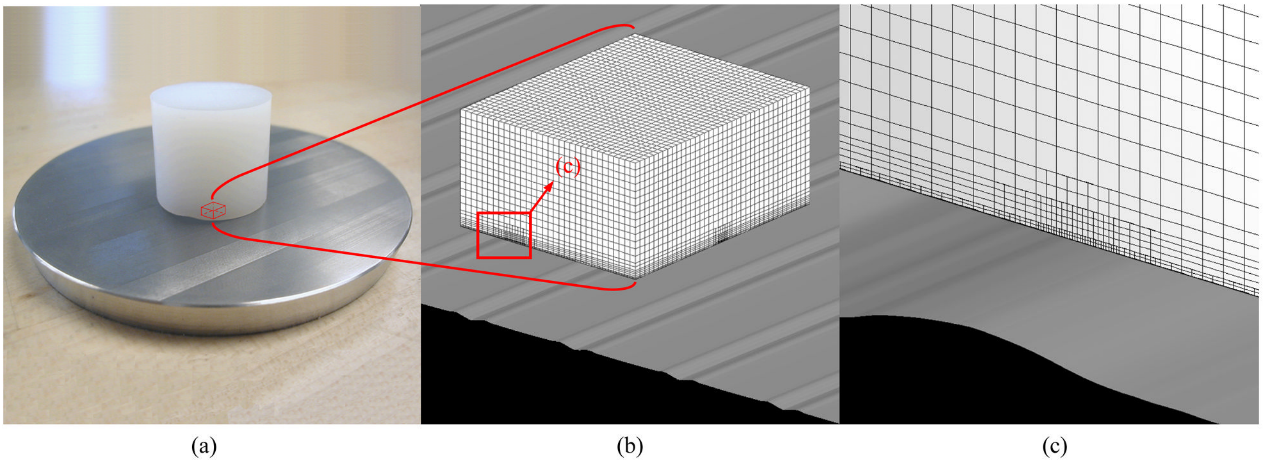

Figure 2.
(A) Pin-plate articulating couple used in polyethylene-stainless steel reciprocating wear tester. The parallel scratches on surface of the metal platen are spaced 150 μm apart. (B) The corresponding polyethylene continuum mesh (white) and analytical scratched stainless steel surface (gray) utilized in the finite element model. (C) Enlarged view illustrating the spatial refinement of the polyethylene mesh in the region used for data registry.

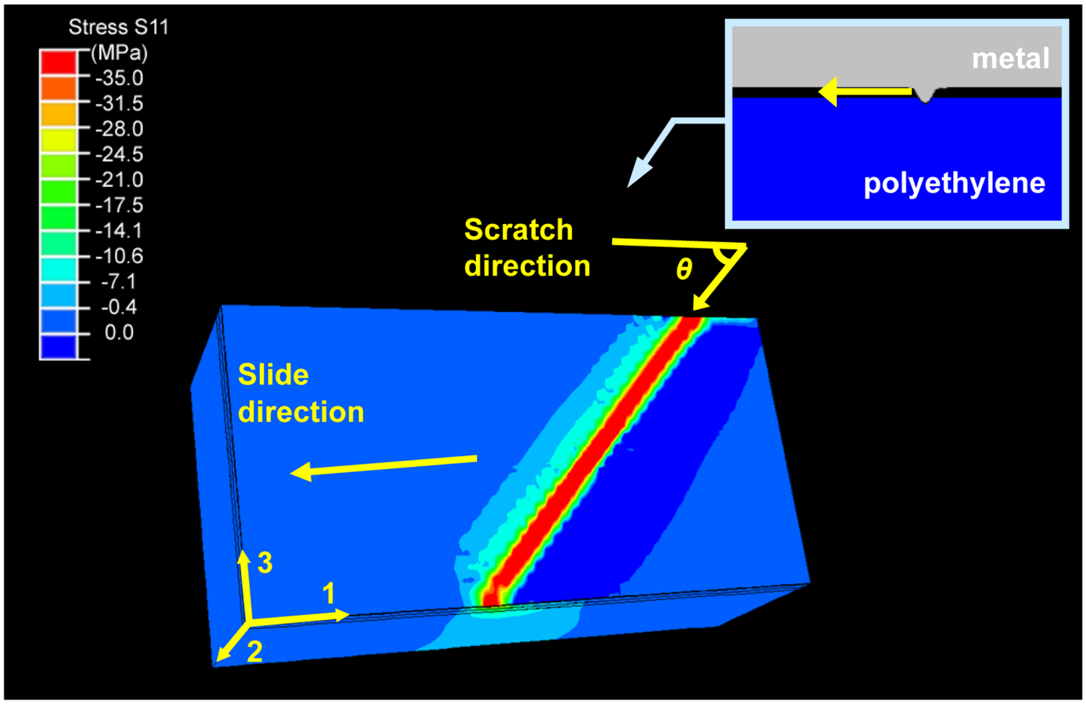

Figure 3.
Contour plot of instantaneous longitudinal normal stress during passage of a scratch oriented at 45°. Note the edge effect near the sides of the block. Fiducial nodes for stress registry were therefore located along the block centerline.

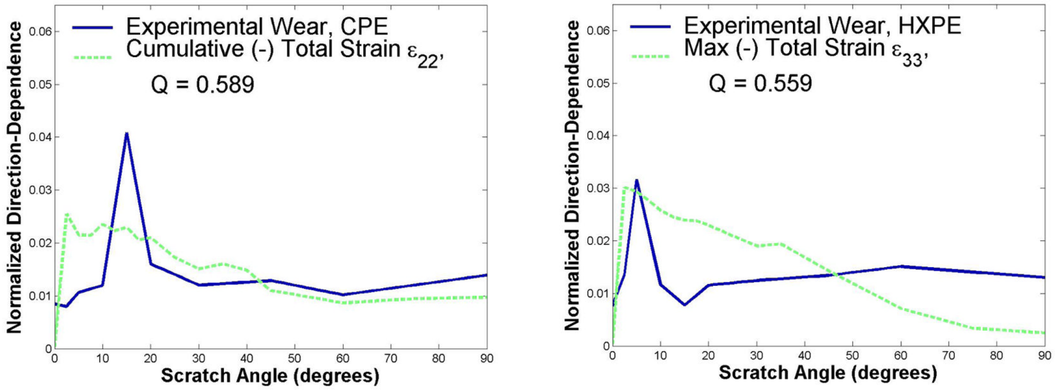

Figure 4.
The two surrogate mechanical stimuli judged to best resemble the scratch lip direction-dependence of experimental wear. "Total strain" refers to the sum of elastic and plastic strain in the specified component direction.

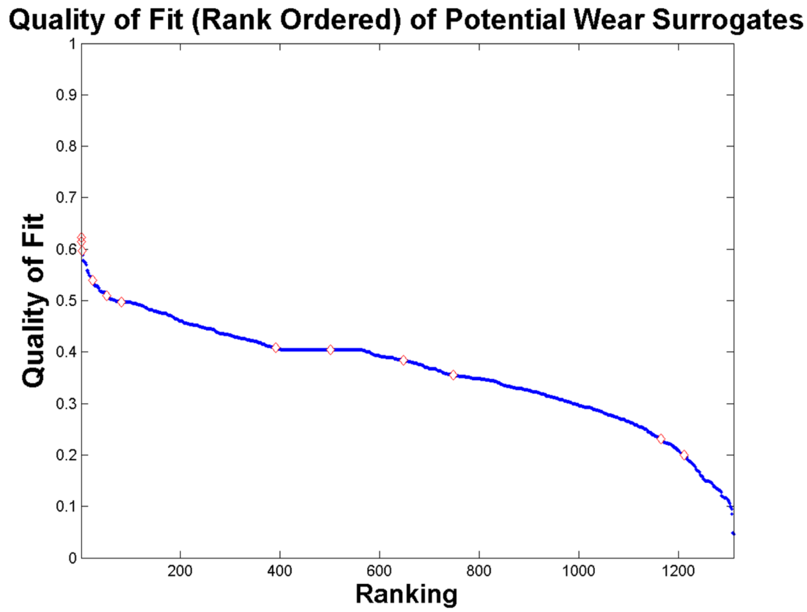

Figure 5.

Statistical fit distribution for all 2,054 comparisons of surrogate candidates to experimental wear. Selected cases (red dots) are illustrated in Figure 6, in order of decreasing quality of fit. Note: after the worst-fitting candidate listed above (#1310, quality of fit = 0.046), for administrative/procedural reasons, all remaining candidates involved incomplete datasets, and were assigned a quality of fit = 0.

NIH-PA Author Manuscript
NIH-PA Author Manuscript

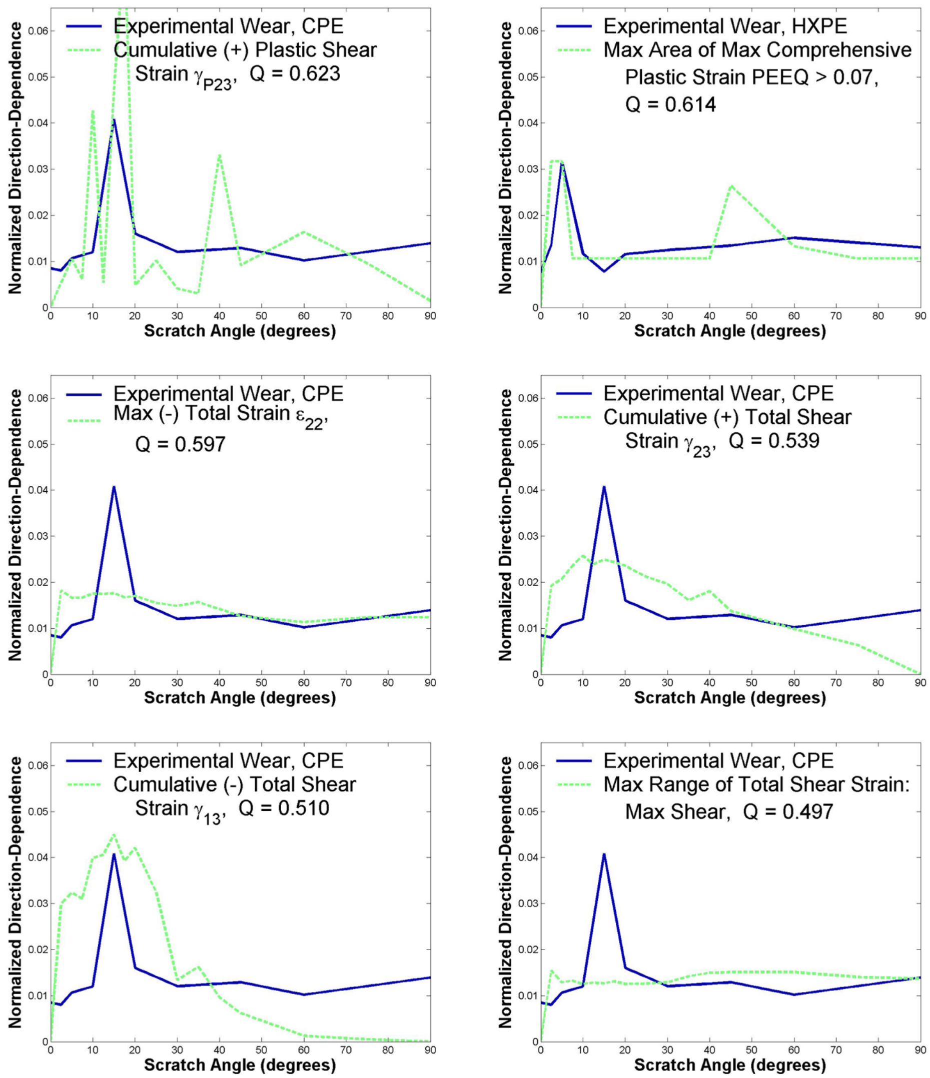

NIH-PA Author Manuscript
NIH-PA Author Manuscript

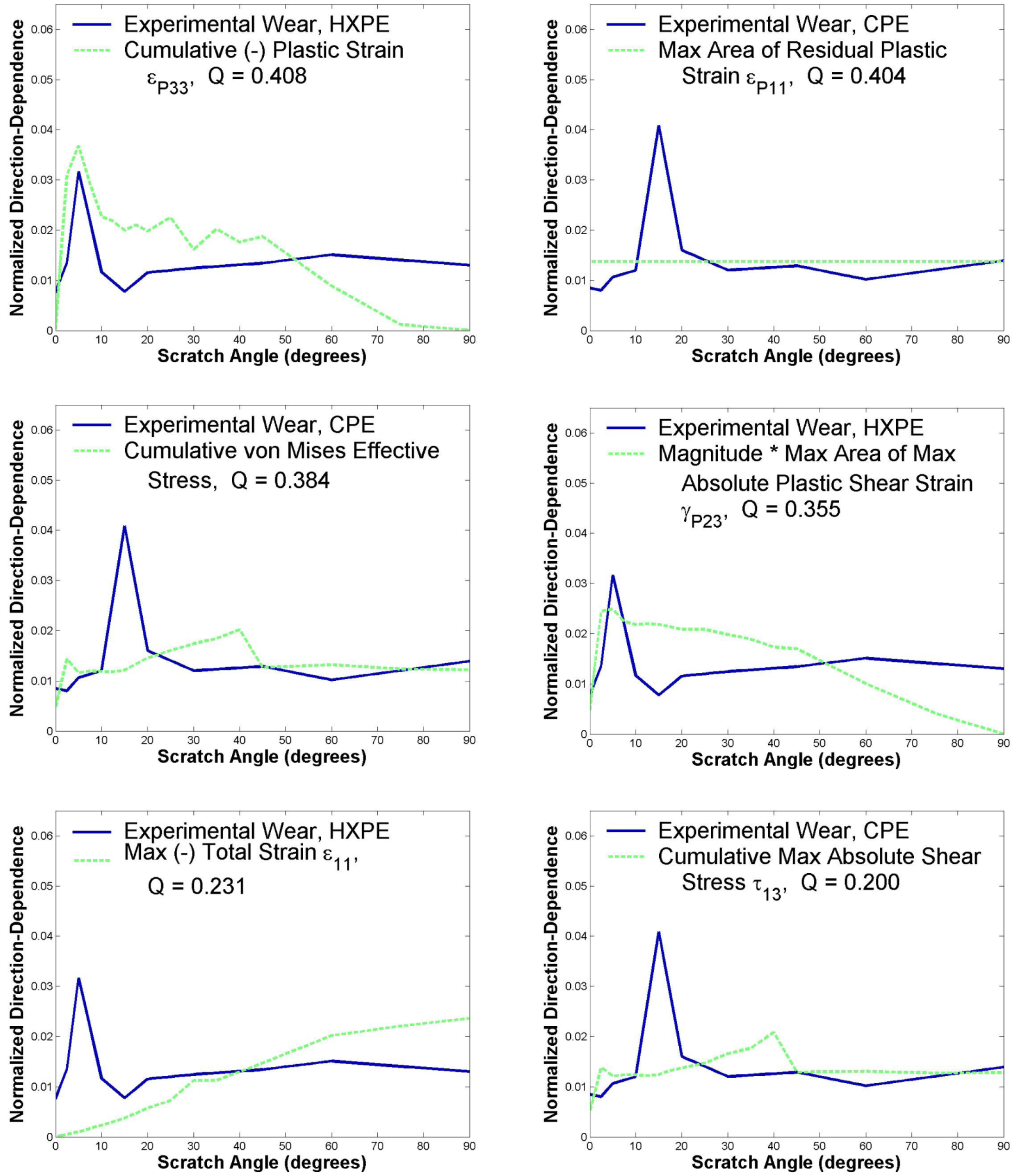

Figure 6.

Selected plots of computational surrogate candidates representing a variety of mechanical stimuli and a range of statistical fit quality. These twelve plots correspond to the respective symbols on the distribution curve in Figure 5.

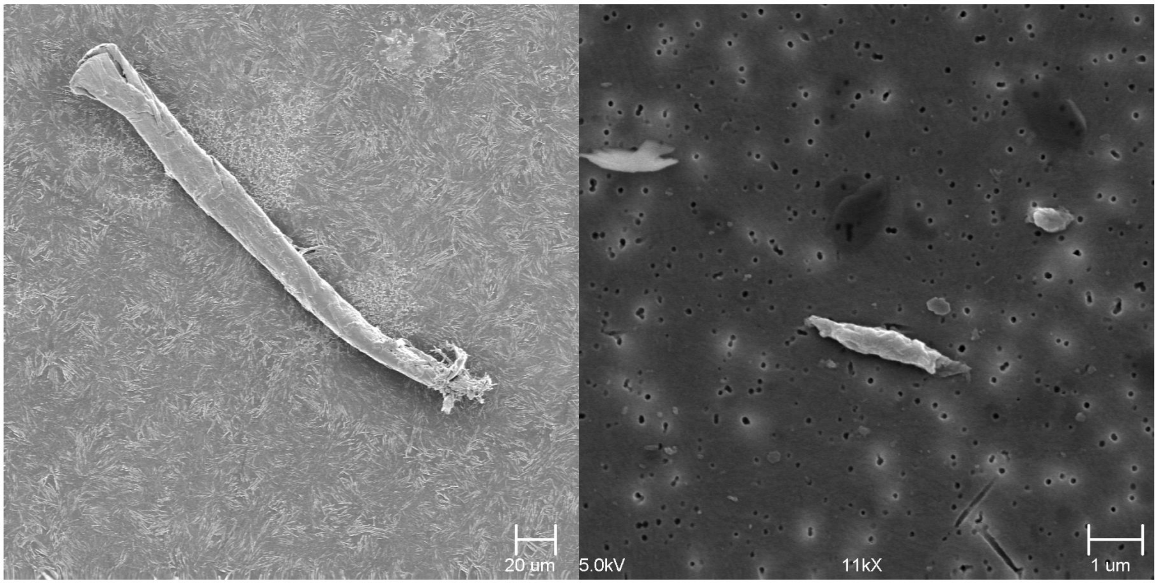

Figure 7.
UHMWPE debris particles collected from the experimental apparatus following articulation. (a) Particles generated by a scratched surface were typically orders larger than the most biologically reactive submicron debris. Here, a particle of crosslinked UHMWPE is presented, produced by a scratch orientation of 5°. (b) A smooth articulation couple produced debris that were of submicron- or micron-order size, similar to the overwhelming volumetric fraction of particles found in tissues surrounding an implanted total joint *in vivo*. Further details regarding the relationships between local stress fields and sliding parameters are reported elsewhere[26].

Table 1

Best-performing 2.5% of the fits for the 2,054 mechanical stimulus candidates to experimentally observed UHMWPE wear (1,027 each for conventional and crosslinked UHMWPE). The tabulated quality of fit Q is the average of three measures: (1) 2-D correlation coefficient r, (2) fraction of shared area $\hat{A}$ in normalized plots of the two given datasets, and (3) correlative statistic R^2 from a fixed/random effects ANOVA statistical model (See Appendix A). The complete rank list is provided in Appendix B (page 30). Please refer to the key following table for abbreviations.

Rank	Q	Stm	TD	Cmp	Rgy	Thrsh	Mtl	Rank	Q	Stm	TD	Cmp	Rgy	Thrsh	Mtl
1	0.623	PS	H	23	(+)		V	36	0.525	APS	I	22	Mx+	0.002	X
2	0.614	APS	I	“E”		0.07	X	37	0.525	TS	I	23	Mx+		V
3	0.597	TS	I	22	Mx−		V	38	0.519	APS	I	MnP	|M|	0.005	X
4	0.589	TS	H	22	(−)		V	39	0.519	APS	I	MnP	Mx−	0.005	X
5	0.578	APS	I	MnP	|M|	0.009	X	40	0.518	TS	I	MxP	|M|		X
6	0.578	APS	I	MnP	Mx−	0.009	X	41	0.518	TS	I	MxP	Mx+		X
7	0.576	TS	I	22	PV		V	42	0.518	APS	I	“M”		0.006	X
8	0.575	APS	I	MxS		0.009	X	43	0.517	APS	I	MxP	|M|	0.005	X
9	0.573	APS	I	MxP	|M|	0.009	X	44	0.517	APS	I	MxP	Mx+	0.005	X
10	0.573	APS	I	MxP	Mx+	0.009	X	45	0.517	PSE	I	Gnl			X
11	0.569	APS	I	MnP	|M|	0.01	X	46	0.516	APS	I	MxP	Mx−	0.0005	V
12	0.569	APS	I	MnP	Mx−	0.01	X	47	0.516	APS	I	MnP	Mx+	0.0005	V
13	0.559	TS	I	33	|M|		X	48	0.516	APS	I	MnP	Mx+	0.005	V
14	0.559	TS	I	33	Mx−		X	49	0.516	M*A	I	MnP	|M|	0	X
15	0.556	APS	I	“E”		0.05	X	50	0.516	M*A	I	MnP	Mx−	0	X
16	0.553	APS	I	MxS		0.02	X	51	0.514	APS	I	MxS		0.005	X
17	0.549	APS	I	11	Mx+	0.0005	V	52	0.511	TS	I	13	Mx−		V
18	0.548	TS	I	MnP	|M|		X	53	0.510	TS	H	13	(−)		V
19	0.548	TS	I	MnP	Mx−		X	54	0.508	APS	I	22	Mx−	0.006	V
20	0.546	M*A	I	“E”		0	X	55	0.506	APS	I	MxP	Mx−	0.001	V
21	0.546	TS	I	23	|M|		X	56	0.505	APS	I	MxP	Mx−	0.002	V
22	0.541	APS	I	MxP	|M|	0.03	X	57	0.504	APS	I	“M”		0.02	X
23	0.541	APS	I	MxP	Mx+	0.03	X	58	0.504	APS	I	MnP	Mx+	0.002	V
24	0.539	TS	H	23	(+)		V	59	0.504	APS	I	MxS		0.03	X
25	0.537	TS	I	MxS			X	60	0.503	M*A	I	MxS		0	X
26	0.535	APS	I	MxS		0.006	X	61	0.503	APS	I	“E”		0.007	X
27	0.531	PS	I	23	Mx+		V	62	0.503	APS	I	MnP	|M|	0.02	X
28	0.531	APS	I	“M”		0.007	X	63	0.503	APS	I	MnP	Mx−	0.02	X
29	0.529	APS	I	MnP	|M|	0.006	X	64	0.503	APS	I	“E”		0.006	X
30	0.529	APS	I	MnP	Mx−	0.006	X	65	0.502	S	H	22	(−)		X
31	0.529	S	I	22	Mx+		X	66	0.502	S	I	23	|M|		X
32	0.528	APS	I	12	Mx−	0.002	V	67	0.502	S	I	23	Mx+		X
33	0.528	APS	I	22	Mx+	0.001	V	68	0.502	APS	I	“M”		0.03	X
34	0.528	APS	I	MnP	Mx+	0.001	V	69	0.500	APS	I	“E”		0.03	X
35	0.526	APS	I	12	Mx−	0.001	V	70	0.500	S	H	3rd	(−)		X

NOTE: The following key provides abbreviations used for the above column headings and corresponding variants: **Q** = **Quality of fit (= 1/3($r + \hat{A} + R^2$)); Stm = Stimulus**; APS = Area of Plastic Strain; MA = Magnitude of Area of plastic strain; PS = Plastic Strain; PSE = Plastic Strain Energy; TS = Total Strain; TSE = Total Strain Energy; **TD** = **Temporal Designation**; I = Instantaneous; H = (Cumulative) History; **Cmp = Component**; 11 = stimulus in the 1-plane, and in the 1-direction; $3^{rd} = 3^{rd}$ Invariant of stress (determinant of the stress tensor); “E” = “Equivalent” (ABAQUS effective value for consolidated tensorial components); Gnl = General state (normal state plus shear state); “M” = “Magnitude” (ABAQUS effective magnitude for consolidated tensorial components); MnP = Min Principal; MxP = Max Principal; Nml = Normal state; prs = equivalent pressure; Shr = Shear state; Tca = Tresca effective stress; vM = von Mises effective stress; **Rgy** = **Registry**; (+) = Positive values; (−) = Negative values; Mx+ = Max positive; Mx− = Max negative; |M| = Max (instantaneous) absolute magnitude; |m| = max (cumulative) absolute magnitude; PV = max cyclic Peak-to-Valley swing (suggestive of a fatigue measure for failure); Res = Residual (plastic strain); **Thrsh** = **Threshold (of plastic strain, used in computing an area of plastic strain); Mtl** = **Material**; V = conventional UHMWPE; X = highly crosslinked UHMWPE.

Appendix B

Complete listing of all ranked candidate surrogates for scratch angle-dependent wear. Please refer to Table 1 key for abbreviations.

Rank	Stm	TD	Cmp	Rgy	Thrsh	Mtl	Q	Rank	Stm	TD	Cmp	Rgy	Thrsh	Mtl	Q
1	PS	H	23	(+)		V	0.623	36	APS	I	22	Mx+	0.002	X	0.525
2	APS	I	“E”		0.07	X	0.614	37	TS	I	23	Mx+		V	0.525
3	TS	I	22	Mx−		V	0.597	38	APS	I	MnP	|M|	0.005	X	0.519
4	TS	H	22	(−)		V	0.589	39	APS	I	MnP	Mx−	0.005	X	0.519
5	APS	I	MnP	|M|	0.009	X	0.578	40	TS	I	MxP	|M|		X	0.518
6	APS	I	MnP	Mx−	0.009	X	0.578	41	TS	I	MxP	Mx+		X	0.518
7	TS	I	22	PV		V	0.576	42	APS	I	“M”		0.006	X	0.518
8	APS	I	MxS		0.009	X	0.575	43	APS	I	MxP	|M|	0.005	X	0.517
9	APS	I	MxP	|M|	0.009	X	0.573	44	APS	I	MxP	Mx+	0.005	X	0.517
10	APS	I	MxP	Mx+	0.009	X	0.573	45	PSE	I	Gnl			X	0.517
11	APS	I	MnP	|M|	0.01	X	0.569	46	APS	I	MxP	Mx−	0.0005	V	0.516
12	APS	I	MnP	Mx−	0.01	X	0.569	47	APS	I	MnP	Mx+	0.0005	V	0.516
13	TS	I	33	|M|		X	0.559	48	APS	I	MnP	Mx+	0.005	V	0.516
14	TS	I	33	Mx−		X	0.559	49	M*A	I	MnP	|M|	0	X	0.516
15	APS	I	“E”		0.05	X	0.556	50	M*A	I	MnP	Mx−	0	X	0.516
16	APS	I	MxS		0.02	X	0.553	51	APS	I	MxS		0.005	X	0.514
17	APS	I	11	Mx+	0.0005	V	0.549	52	TS	I	13	Mx−		V	0.511
18	TS	I	MnP	|M|		X	0.548	53	TS	H	13	(−)		V	0.510
19	TS	I	MnP	Mx−		X	0.548	54	APS	I	22	Mx−	0.006	V	0.508
20	M*A	I	“E”		0	X	0.546	55	APS	I	MxP	Mx−	0.001	V	0.506
21	TS	I	23	|M|		X	0.546	56	APS	I	MxP	Mx−	0.002	V	0.505
22	APS	I	MxP	|M|	0.03	X	0.541	57	APS	I	“M”		0.02	X	0.504
23	APS	I	MxP	Mx+	0.03	X	0.541	58	APS	I	MnP	Mx+	0.002	V	0.504
24	TS	H	23	(+)		V	0.539	59	APS	I	MxS		0.03	X	0.504
25	TS	I	MxS			X	0.537	60	M*A	I	MxS		0	X	0.503
26	APS	I	MxS		0.006	X	0.535	61	APS	I	“E”		0.007	X	0.503
27	PS	I	23	Mx+		V	0.531	62	APS	I	MnP	|M|	0.02	X	0.503
28	APS	I	“M”		0.007	X	0.531	63	APS	I	MnP	Mx−	0.02	X	0.503
29	APS	I	MnP	|M|	0.006	X	0.529	64	APS	I	“E”		0.006	X	0.503
30	APS	I	MnP	Mx−	0.006	X	0.529	65	S	H	22	(−)		X	0.502
31	S	I	22	Mx+		X	0.529	66	S	I	23	|M|		X	0.502
32	APS	I	12	Mx−	0.002	V	0.528	67	S	I	23	Mx+		X	0.502
33	APS	I	22	Mx+	0.001	V	0.528	68	APS	I	“M”		0.03	X	0.502
34	APS	I	MnP	Mx+	0.001	V	0.528	69	APS	I	“E”		0.03	X	0.500
35	APS	I	12	Mx−	0.001	V	0.526	70	S	H	3rd	(−)		X	0.500
71	M*A	I	“M”		0	X	0.499	121	S	I	prs	PV		X	0.491
72	S	I	3rd	|M|		X	0.499	122	S	I	11	PV		X	0.490
73	S	I	3rd	Mx−		X	0.499	123	S	I	33	|M|		X	0.490
74	APS	I	12	Mx−	0.0005	X	0.499	124	S	I	33	Mx−		X	0.490
75	S	H	33	(+)		V	0.498	125	TSE	I	Shr			X	0.489
76	APS	I	“E”		0.04	X	0.498	126	APS	I	11	Res	0.0005	V	0.489
77	TS	I	33	PV		X	0.498	127	S	I	MxP	PV		X	0.489
78	APS	I	MnP	|M|	0.03	X	0.497	128	S	I	MxP	|M|		X	0.488
79	APS	I	MnP	Mx−	0.03	X	0.497	129	S	I	MxP	Mx−		X	0.488
80	APS	I	“E”		0.06	X	0.497	130	M*A	I	22	Mx−	0	V	0.486
81	PSE	I	Shr	PV		X	0.497	131	S	H	prs	(+)		X	0.486
82	TS	I	MxS	PV		X	0.497	132	S	I	22	PV		X	0.486
83	APS	I	12	|M|	0.0005	X	0.497	133	APS	I	MxP	Mx−	0.003	V	0.485
84	APS	I	12	Mx+	0.0005	X	0.497	134	APS	I	MnP	Mx+	0.003	V	0.485
85	TSE	I	Shr	PV		X	0.497	135	APS	I	22	Mx−	0.01	V	0.483
86	TS	I	23	PV		X	0.497	136	TS	I	22	|M|		X	0.483
87	TS	I	MnP	PV		X	0.497	137	PS	I	MnP	PV		X	0.482
88	S	I	Tca	PV		X	0.497	138	APS	I	“M”		0.04	X	0.482
89	S	I	vM	PV		X	0.497	139	APS	I	11	|M|	0.0005	V	0.482

Rank	Stm	TD	Cmp	Rgy	Thrsh	Mtl	Q	Rank	Stm	TD	Cmp	Rgy	Thrsh	Mtl	Q
90	S	I	3rd	PV		X	0.497	140	S	I	MxS			X	0.482
91	S	I	MxS	PV		X	0.497	141	S	I	Tca			X	0.482
92	S	I	23	PV		X	0.497	142	S	I	vM			X	0.482
93	TSE	I	Nml			X	0.497	143	TS	I	22	Mx+		X	0.482
94	APS	I	22	|M|	0.004	V	0.497	144	S	H	prs	(−)		X	0.482
95	TSE	I	Gnl			X	0.497	145	TS	I	22	Mx−		X	0.481
96	PSE	I	Gnl	PV		X	0.497	146	APS	I	MxP	Mx−	0.004	V	0.480
97	TS	H	33	(−)		V	0.497	147	S	H	3rd	(+)		V	0.480
98	S	I	MnP	|M|		X	0.497	148	APS	I	12	|M|	0.002	V	0.480
99	S	I	MnP	Mx−		X	0.497	149	APS	I	12	Mx+	0.002	V	0.480
100	APS	I	12	Mx−	0.0005	V	0.497	150	APS	I	MnP	Mx+	0.004	V	0.480
101	APS	I	22	Mx−	0.004	V	0.496	151	PS	I	“M”	PV		X	0.479
102	S	I	MnP	PV		X	0.496	152	TS	I	23	Mx+		X	0.479
103	S	I	3rd	Mx+		X	0.496	153	APS	I	MxP	Mx−	0.005	V	0.478
104	S	I	22	|M|		X	0.495	154	S	H	33	(−)		X	0.478
105	S	I	22	Mx−		X	0.495	155	APS	I	12	|M|	0.001	X	0.478
106	S	I	33	Mx+		X	0.495	156	APS	I	12	Mx+	0.001	X	0.478
107	TSE	I	Nml	PV		X	0.495	157	PSE	I	Nml			X	0.477
108	TS	I	MxP	PV		X	0.494	158	APS	I	MxP	|M|	0.004	X	0.477
109	TSE	I	Gnl	PV		X	0.494	159	APS	I	“M”		0.005	X	0.477
110	S	I	33	PV		X	0.494	160	APS	I	MxS		0.004	X	0.477
111	TS	I	22	PV		X	0.494	161	APS	I	MxP	Mx+	0.004	X	0.477
112	APS	I	22	Mx−	0.009	V	0.493	162	APS	I	MxP	|M|	0.006	X	0.476
113	S	I	11	|M|		X	0.493	163	APS	I	MxP	Mx+	0.006	X	0.476
114	S	I	11	Mx−		X	0.493	164	PS	I	MxS	PV		X	0.476
115	S	H	23	(−)		V	0.493	165	APS	I	22	Mx+	0.0005	V	0.476
116	S	H	3rd	(+)		X	0.492	166	S	H	12			X	0.476
117	S	I	prs	|M|		X	0.492	167	S	I	MxP	Mx+		V	0.475
118	S	I	prs	Mx+		X	0.492	168	TS	I	23	PV		V	0.475
119	M*A	I	MxP	|M|	0	X	0.492	169	PSE	I	Nml	PV		X	0.475
120	M*A	I	MxP	Mx+	0	X	0.492	170	TS	I	33	|M|		V	0.475
171	TS	I	33	Mx−		V	0.475	221	APS	I	“E”		0.03	V	0.454
172	S	H	11	(−)		X	0.475	222	APS	I	MxP	|M|	0.02	X	0.454
173	TS	I	23	Mx−		X	0.474	223	APS	I	MxP	Mx+	0.02	X	0.454
174	PS	I	MxP	PV		X	0.473	224	APS	I	22	|M|	0.01	V	0.454
175	TS	I	33	PV		V	0.473	225	PS	I	33	|M|		X	0.453
176	APS	I	“E”		0.008	X	0.472	226	APS	I	“E”		0.04	V	0.452
177	S	I	23	|M|		V	0.471	227	TS	I	23	|M|		V	0.452
178	S	I	23	Mx+		V	0.471	228	TS	I	23	Mx−		V	0.452
179	S	I	prs	Mx−		V	0.471	229	APS	I	MnP	|M|	0.03	V	0.452
180	S	I	33	Mx+		V	0.471	230	APS	I	12	|M|	0.0005	V	0.452
181	TS	H	12	(+)		X	0.471	231	APS	I	MnP	Mx−	0.03	V	0.452
182	S	I	3rd	|M|		V	0.470	232	APS	I	“E”		0.06	V	0.452
183	S	I	3rd	Mx−		V	0.470	233	APS	I	12	Mx+	0.0005	V	0.452
184	APS	I	12	|M|	0.003	V	0.469	234	S	I	13	Mx−		V	0.452
185	APS	I	12	Mx+	0.003	V	0.469	235	S	I	23	Mx−		X	0.452
186	APS	I	12	|M|	0.001	V	0.467	236	S	I	33	PV		V	0.451
187	APS	I	12	Mx+	0.001	V	0.467	237	S	I	23	Mx−		V	0.451
188	PS	I	12	PV		X	0.466	238	S	I	12	PV		X	0.450
189	S	H	23	(+)		V	0.465	239	APS	I	23	|M|	0.008	V	0.450
190	APS	I	22	|M|	0.009	V	0.465	240	APS	I	23	Mx−	0.008	V	0.450
191	S	I	MxP	Mx+		X	0.465	241	APS	I	MxS		0.03	V	0.449
192	APS	I	MnP	Mx+	0.006	V	0.464	242	APS	I	23	|M|	0.01	V	0.448
193	APS	I	22	|M|	0.006	V	0.464	243	APS	I	23	Mx−	0.01	V	0.448
194	S	I	3rd	PV		V	0.463	244	APS	I	23	|M|	0.007	V	0.448
195	APS	I	12	Mx−	0.001	X	0.463	245	APS	I	23	Mx−	0.007	V	0.448

Rank	Stm	TD	Cmp	Rgy	Thrsh	Mtl	Q	Rank	Stm	TD	Cmp	Rgy	Thrsh	Mtl	Q
196	APS	I	MxS		0.01	X	0.463	246	APS	I	22	Mx−	0.008	V	0.448
197	S	I	23	PV		V	0.462	247	APS	I	33	Mx−	0.001	V	0.448
198	PS	I	“E”	PV		X	0.461	248	APS	I	33	|M|	0.002	V	0.447
199	APS	I	MxP	|M|	0.01	X	0.461	249	APS	I	33	Mx+	0.002	V	0.447
200	APS	I	MxP	Mx+	0.01	X	0.461	250	APS	I	33	|M|	0.003	V	0.447
201	APS	I	22	Mx−	0.005	V	0.460	251	APS	I	33	Mx+	0.003	V	0.447
202	APS	I	33	Mx−	0.0005	V	0.460	252	S	I	Tca	PV		V	0.445
203	S	H	12	(+)		X	0.460	253	S	I	MxS	PV		V	0.445
204	M*A	I	23	|M|	0	V	0.460	254	TS	I	12	PV		X	0.445
205	M*A	I	23	Mx−	0	V	0.460	255	APS	I	MxP	|M|	0.006	V	0.445
206	PS	H	22	(+)		X	0.458	256	APS	I	MxP	Mx+	0.006	V	0.445
207	TS	H	33			V	0.457	257	S	I	vM	PV		V	0.445
208	APS	I	“E”		0.007	V	0.457	258	PS	I	11	PV		X	0.445
209	APS	I	MnP	|M|	0.02	V	0.457	259	S	H	13	(−)		V	0.445
210	APS	I	MnP	Mx−	0.02	V	0.457	260	APS	I	23	|M|	0.009	V	0.445
211	APS	I	“E”		0.006	V	0.457	261	APS	I	23	Mx−	0.009	V	0.445
212	APS	I	33	Mx+	0.001	V	0.456	262	TS	I	33	Mx+		V	0.445
213	APS	I	“M”		0.03	V	0.456	263	TSE	H	Shr			V	0.444
214	S	H	33	(+)		X	0.455	264	TSE	I	Gnl			V	0.444
215	S	I	3rd	Mx+		V	0.455	265	PS	I	13	|M|		V	0.444
216	APS	I	MxP	Mx−	0.006	V	0.455	266	PS	I	13	Mx+		V	0.444
217	APS	I	33	|M|	0.001	V	0.455	267	PS	I	MxP	|M|		X	0.444
218	TS	I	33	Mx+		X	0.454	268	PS	I	MxP	Mx+		X	0.444
219	S	H	33	(−)		V	0.454	269	APS	I	22	|M|	0.02	X	0.442
220	S	H	12			V	0.454	270	APS	I	MxS		0.005	V	0.442
271	APS	I	23	Mx+	0.0005	V	0.440	321	S	H	22	(−)		V	0.427
272	M*A	I	22	|M|	0	V	0.439	322	PS	I	MnP	|M|		V	0.427
273	APS	I	23	Mx+	0.002	V	0.439	323	PS	I	MnP	Mx−		V	0.427
274	APS	I	23	Mx+	0.001	V	0.438	324	S	I	prs	|M|		V	0.426
275	PS	I	22	PV		X	0.438	325	S	I	prs	Mx+		V	0.426
276	APS	I	“M”		0.008	V	0.437	326	APS	I	13	|M|	0.0005	V	0.426
277	S	H	22	(+)		X	0.437	327	APS	I	22	|M|	0.003	X	0.426
278	S	I	11	Mx+		V	0.437	328	M*A	I	33	Mx+	0	V	0.426
279	APS	I	13	Mx−	0.001	V	0.436	329	APS	I	33	|M|	0.0005	V	0.426
280	APS	I	13	|M|	0.001	V	0.436	330	TS	I	13	Mx−		X	0.426
281	TSE	I	Nml			V	0.436	331	APS	I	33	Mx+	0.0005	V	0.425
282	PS	I	33	PV		V	0.436	332	APS	I	“E”		0.02	X	0.425
283	APS	I	“E”		0.008	V	0.436	333	APS	I	22	|M|	0.005	X	0.425
284	APS	I	23	|M|	0.03	V	0.436	334	TSE	I	Shr	PV		V	0.424
285	APS	I	23	Mx−	0.03	V	0.436	335	S	I	13	PV		V	0.424
286	PS	I	33	|M|		V	0.436	336	APS	I	33	Mx+	0.005	V	0.423
287	PS	I	22	Mx+		X	0.436	337	S	I	prs	Mx−		X	0.423
288	TSE	I	Gnl	PV		V	0.435	338	S	H	prs	(+)		V	0.423
289	APS	I	MnP	|M|	0.007	V	0.435	339	S	I	12	Mx+		X	0.423
290	APS	I	MnP	Mx−	0.007	V	0.435	340	M*A	I	33	|M|	0	V	0.422
291	APS	I	MxP	|M|	0.005	V	0.435	341	TS	H	33	(+)		V	0.422
292	APS	I	MxP	Mx+	0.005	V	0.435	342	APS	I	MxP	Mx−	0.0005	X	0.422
293	S	I	MxP	PV		V	0.434	343	APS	I	MnP	Mx+	0.0005	X	0.422
294	S	I	vM			V	0.434	344	TS	I	12	|M|		X	0.422
295	S	I	MxS			V	0.434	345	TS	I	12	Mx+		X	0.422
296	S	I	Tca			V	0.434	346	APS	I	22	Mx+	0.006	X	0.422
297	S	I	prs	PV		V	0.433	347	APS	I	23	Mx+	0.004	V	0.422
298	APS	I	MxS		0.007	V	0.433	348	S	I	MxP	|M|		V	0.421
299	APS	I	13	Mx−	0.0005	V	0.433	349	S	I	MxP	Mx−		V	0.421
300	S	I	MnP	|M|		V	0.433	350	APS	I	23	|M|	0.05	V	0.421
301	S	I	MnP	Mx−		V	0.433	351	APS	I	23	Mx−	0.05	V	0.421

Rank	Stm	TD	Cmp	Rgy	Thrsh	Mtl	Q	Rank	Stm	TD	Cmp	Rgy	Thrsh	Mtl	Q
302	TS	H	23	(−)		V	0.432	352	PSE	I	Shr	PV		V	0.421
303	PS	I	MxS			X	0.432	353	PS	I	33	Mx−		X	0.421
304	APS	I	“M”		0.006	V	0.432	354	S	I	11	PV		V	0.420
305	S	I	MnP	PV		V	0.432	355	APS	I	12	Mx−	0.003	V	0.419
306	S	I	22	Mx+		V	0.430	356	TS	I	13	PV		X	0.419
307	APS	I	23	Mx+	0.008	V	0.430	357	APS	I	22	Mx−	0.003	V	0.418
308	TSE	I	Nml	PV		V	0.430	358	PS	I	12	|M|		V	0.418
309	APS	I	13	Mx+	0.001	X	0.429	359	PS	I	12	Mx+		V	0.418
310	S	I	22	PV		V	0.429	360	APS	I	MnP	|M|	0.006	V	0.418
311	S	I	22	|M|		V	0.429	361	APS	I	MnP	Mx−	0.006	V	0.418
312	S	I	22	Mx−		V	0.429	362	PS	I	“M”			X	0.418
313	S	I	33	|M|		V	0.429	363	PS	I	MnP	PV		V	0.416
314	S	I	33	Mx−		V	0.429	364	TS	I	11	PV		X	0.416
315	PS	I	13	PV		V	0.429	365	PS	H	22			X	0.416
316	TS	H	22	(+)		X	0.428	366	APS	I	“M”		0.007	V	0.415
317	PS	I	33	Mx−		V	0.428	367	APS	I	22	|M|	0.005	V	0.415
318	APS	I	“E”		0.05	V	0.428	368	TS	I	13	PV		V	0.415
319	TS	H	12			X	0.428	369	APS	I	33	|M|	0.005	V	0.415
320	APS	I	13	Mx+	0.0005	V	0.428	370	APS	I	“E”		0.009	V	0.414
371	TS	H	23	|m|		X	0.413	421	APS	I	13	Res	0	X	0.404
372	APS	I	23	Mx+	0.006	V	0.413	422	APS	I	12	Res	0	X	0.404
373	S	I	13	PV		X	0.413	423	APS	I	MnP	Res	0	X	0.404
374	APS	I	23	|M|	0.006	V	0.412	424	APS	I	MxP	Res	0	X	0.404
375	APS	I	23	Mx−	0.006	V	0.412	425	APS	I	33	Res	0	X	0.404
376	APS	I	22	Mx−	0.003	X	0.412	426	APS	I	22	Res	0	X	0.404
377	APS	I	23	Mx+	0.003	V	0.412	427	APS	I	11	Res	0	X	0.404
378	APS	I	MnP	Mx+	0.001	X	0.412	428	APS	I	MnP	|M|	0.004	X	0.404
379	APS	I	23	Mx+	0.007	V	0.412	429	APS	I	MnP	|M|	0.003	X	0.404
380	APS	I	22	|M|	0.008	X	0.411	430	APS	I	MxP	|M|	0.003	X	0.404
381	M*A	I	23	Mx+	0	V	0.411	431	APS	I	MnP	|M|	0.002	X	0.404
382	S	I	11	|M|		V	0.410	432	APS	I	MxP	|M|	0.002	X	0.404
383	S	I	11	Mx−		V	0.410	433	APS	I	22	|M|	0.002	X	0.404
384	APS	I	“M”		0.01	X	0.410	434	APS	I	MnP	|M|	0.001	X	0.404
385	PS	I	33	PV		X	0.410	435	APS	I	MxP	|M|	0.001	X	0.404
386	TS	H	13	|m|		X	0.409	436	APS	I	22	|M|	0.001	X	0.404
387	PS	I	MxS			V	0.409	437	APS	I	MnP	|M|	0.0005	X	0.404
388	PS	I	“M”			V	0.409	438	APS	I	MxP	|M|	0.0005	X	0.404
389	PS	I	23	|M|		V	0.408	439	APS	I	22	|M|	0.0005	X	0.404
390	PS	I	23	Mx−		V	0.408	440	APS	I	23	|M|	0	X	0.404
391	PS	H	33	(−)		X	0.408	441	APS	I	13	|M|	0	X	0.404
392	APS	I	22	|M|	0.003	V	0.407	442	APS	I	12	|M|	0	X	0.404
393	APS	I	MxS		0.006	V	0.407	443	APS	I	MnP	|M|	0	X	0.404
394	PS	I	“E”			V	0.407	444	APS	I	MxP	|M|	0	X	0.404
395	APS	I	23	|M|	0.005	V	0.407	445	APS	I	33	|M|	0	X	0.404
396	APS	I	23	Mx−	0.005	V	0.407	446	APS	I	22	|M|	0	X	0.404
397	PS	I	“E”	PV		V	0.406	447	APS	I	11	|M|	0	X	0.404
398	PS	I	23	PV		X	0.406	448	APS	I	MnP	Mx−	0.004	X	0.404
399	APS	I	MxS		0.007	X	0.406	449	APS	I	MnP	Mx−	0.003	X	0.404
400	APS	I	MnP	|M|	0.007	X	0.406	450	APS	I	MnP	Mx−	0.002	X	0.404
401	APS	I	MnP	Mx−	0.007	X	0.406	451	APS	I	MnP	Mx−	0.001	X	0.404
402	APS	I	11	Mx+	0.001	X	0.405	452	APS	I	MnP	Mx−	0.0005	X	0.404
403	APS	I	23	|M|	0.003	X	0.405	453	APS	I	23	Mx−	0	X	0.404
404	APS	I	23	Mx−	0.003	X	0.405	454	APS	I	13	Mx−	0	X	0.404
405	APS	I	23	|M|	0.002	X	0.405	455	APS	I	12	Mx−	0	X	0.404
406	APS	I	23	Mx−	0.002	X	0.405	456	APS	I	MnP	Mx−	0	X	0.404
407	APS	I	“M”		0.008	X	0.405	457	APS	I	MxP	Mx−	0	X	0.404

Rank	Stm	TD	Cmp	Rgy	Thrsh	Mtl	Q	Rank	Stm	TD	Cmp	Rgy	Thrsh	Mtl	Q
408	APS	I	23	Mx+	0.009	V	0.405	458	APS	I	33	Mx−	0	X	0.404
409	APS	I	23	Mx−	0.001	X	0.405	459	APS	I	22	Mx−	0	X	0.404
410	APS	I	MxP	Mx−	0.001	X	0.405	460	APS	I	11	Mx−	0	X	0.404
411	APS	I	23	|M|	0.02	V	0.405	461	APS	I	“E”		0.005	X	0.404
412	APS	I	23	Mx−	0.02	V	0.405	462	APS	I	“M”		0.004	X	0.404
413	APS	I	23	Mx+	0.005	V	0.404	463	APS	I	“E”		0.004	X	0.404
414	APS	I	23	|M|	0.0005	X	0.404	464	APS	I	“M”		0.003	X	0.404
415	APS	I	23	Mx−	0.0005	X	0.404	465	APS	I	“E”		0.003	X	0.404
416	APS	I	11	|M|	0.001	X	0.404	466	APS	I	MxS		0.003	X	0.404
417	APS	I	“M”	Res	0	X	0.404	467	APS	I	MxP	Mx+	0.003	X	0.404
418	APS	I	“E”	Res	0	X	0.404	468	APS	I	“M”		0.002	X	0.404
419	APS	I	MxS	Res	0	X	0.404	469	APS	I	“E”		0.002	X	0.404
420	APS	I	23	Res	0	X	0.404	470	APS	I	MxS		0.002	X	0.404
471	APS	I	MxP	Mx+	0.002	X	0.404	521	APS	I	11	|M|	0	V	0.404
472	APS	I	“M”		0.001	X	0.404	522	APS	I	MnP	Mx−	0.004	V	0.404
473	APS	I	“E”		0.001	X	0.404	523	APS	I	MnP	Mx−	0.003	V	0.404
474	APS	I	MxS		0.001	X	0.404	524	APS	I	MnP	Mx−	0.002	V	0.404
475	APS	I	MxP	Mx+	0.001	X	0.404	525	APS	I	MnP	Mx−	0.001	V	0.404
476	APS	I	“M”		0.0005	X	0.404	526	APS	I	MnP	Mx−	0.0005	V	0.404
477	APS	I	“E”		0.0005	X	0.404	527	APS	I	23	Mx−	0	V	0.404
478	APS	I	MxS		0.0005	X	0.404	528	APS	I	13	Mx−	0	V	0.404
479	APS	I	MxP	Mx+	0.0005	X	0.404	529	APS	I	12	Mx−	0	V	0.404
480	APS	I	“M”		0	X	0.404	530	APS	I	MnP	Mx−	0	V	0.404
481	APS	I	“E”		0	X	0.404	531	APS	I	MxP	Mx−	0	V	0.404
482	APS	I	MxS		0	X	0.404	532	APS	I	33	Mx−	0	V	0.404
483	APS	I	23	Mx+	0	X	0.404	533	APS	I	22	Mx−	0	V	0.404
484	APS	I	13	Mx+	0	X	0.404	534	APS	I	11	Mx−	0	V	0.404
485	APS	I	12	Mx+	0	X	0.404	535	APS	I	“E”		0.005	V	0.404
486	APS	I	MnP	Mx+	0	X	0.404	536	APS	I	“M”		0.004	V	0.404
487	APS	I	MxP	Mx+	0	X	0.404	537	APS	I	“E”		0.004	V	0.404
488	APS	I	33	Mx+	0	X	0.404	538	APS	I	“M”		0.003	V	0.404
489	APS	I	22	Mx+	0	X	0.404	539	APS	I	“E”		0.003	V	0.404
490	APS	I	11	Mx+	0	X	0.404	540	APS	I	MxS		0.003	V	0.404
491	APS	I	“M”	Res	0	V	0.404	541	APS	I	MxP	Mx+	0.003	V	0.404
492	APS	I	“E”	Res	0	V	0.404	542	APS	I	“M”		0.002	V	0.404
493	APS	I	MxS	Res	0	V	0.404	543	APS	I	“E”		0.002	V	0.404
494	APS	I	23	Res	0	V	0.404	544	APS	I	MxS		0.002	V	0.404
495	APS	I	13	Res	0	V	0.404	545	APS	I	MxP	Mx+	0.002	V	0.404
496	APS	I	12	Res	0	V	0.404	546	APS	I	“M”		0.001	V	0.404
497	APS	I	MnP	Res	0	V	0.404	547	APS	I	“E”		0.001	V	0.404
498	APS	I	MxP	Res	0	V	0.404	548	APS	I	MxS		0.001	V	0.404
499	APS	I	33	Res	0	V	0.404	549	APS	I	MxP	Mx+	0.001	V	0.404
500	APS	I	22	Res	0	V	0.404	550	APS	I	“M”		0.0005	V	0.404
501	APS	I	11	Res	0	V	0.404	551	APS	I	“E”		0.0005	V	0.404
502	APS	I	MnP	|M|	0.004	V	0.404	552	APS	I	MxS		0.0005	V	0.404
503	APS	I	MnP	|M|	0.003	V	0.404	553	APS	I	MxP	Mx+	0.0005	V	0.404
504	APS	I	MxP	|M|	0.003	V	0.404	554	APS	I	“M”		0	V	0.404
505	APS	I	MnP	|M|	0.002	V	0.404	555	APS	I	“E”		0	V	0.404
506	APS	I	MxP	|M|	0.002	V	0.404	556	APS	I	MxS		0	V	0.404
507	APS	I	22	|M|	0.002	V	0.404	557	APS	I	23	Mx+	0	V	0.404
508	APS	I	MnP	|M|	0.001	V	0.404	558	APS	I	13	Mx+	0	V	0.404
509	APS	I	MxP	|M|	0.001	V	0.404	559	APS	I	12	Mx+	0	V	0.404
510	APS	I	22	|M|	0.001	V	0.404	560	APS	I	MnP	Mx+	0	V	0.404
511	APS	I	MnP	|M|	0.0005	V	0.404	561	APS	I	MxP	Mx+	0	V	0.404
512	APS	I	MxP	|M|	0.0005	V	0.404	562	APS	I	33	Mx+	0	V	0.404
513	APS	I	22	|M|	0.0005	V	0.404	563	APS	I	22	Mx+	0	V	0.404

Rank	Stm	TD	Cmp	Rgy	Thrsh	Mtl	Q	Rank	Stm	TD	Cmp	Rgy	Thrsh	Mtl	Q
514	APS	I	23	|M|	0	V	0.404	564	APS	I	11	Mx+	0	V	0.404
515	APS	I	13	|M|	0	V	0.404	565	APS	I	23	|M|	0.001	X	0.404
516	APS	I	12	|M|	0	V	0.404	566	APS	I	11	Res	0.001	X	0.403
517	APS	I	MnP	|M|	0	V	0.404	567	APS	I	23	|M|	0.004	V	0.403
518	APS	I	MxP	|M|	0	V	0.404	568	APS	I	23	Mx−	0.004	V	0.403
519	APS	I	33	|M|	0	V	0.404	569	APS	I	22	Mx+	0.008	X	0.403
520	APS	I	22	|M|	0	V	0.404	570	PS	I	“M”	PV		V	0.403
571	PS	I	MxS	PV		V	0.402	621	APS	I	11	Res	0.003	X	0.389
572	APS	I	33	|M|	0.004	V	0.402	622	S	H	13	(+)		V	0.389
573	PS	I	23	PV		V	0.401	623	APS	I	22	Mx−	0.005	X	0.389
574	APS	I	13	Mx+	0.002	V	0.401	624	APS	I	MxP	|M|	0.007	V	0.389
575	APS	I	23	|M|	0.07	X	0.400	625	APS	I	MxP	Mx+	0.007	V	0.389
576	APS	I	23	Mx−	0.07	X	0.400	626	TSE	I	Shr			V	0.389
577	APS	I	33	Mx+	0.004	V	0.400	627	APS	I	33	|M|	0.008	V	0.389
578	S	H	33			V	0.400	628	M*A	I	22	Mx+	0	X	0.388
579	S	I	13	|M|		V	0.400	629	APS	I	33	Mx−	0.002	V	0.387
580	S	H	11	(+)		X	0.400	630	APS	I	13	Mx+	0.003	X	0.387
581	PS	I	MnP	|M|		X	0.398	631	APS	I	22	|M|	0.007	X	0.387
582	PS	I	MnP	Mx−		X	0.398	632	S	H	22			V	0.387
583	PS	H	12	(+)		X	0.397	633	S	H	MnP			V	0.387
584	APS	I	33	Mx+	0.008	V	0.396	634	PS	I	MxP	PV		V	0.387
585	APS	I	23	|M|	0.004	X	0.396	635	APS	I	33	|M|	0.0005	X	0.386
586	APS	I	23	Mx−	0.004	X	0.396	636	APS	I	33	Mx+	0.0005	X	0.386
587	APS	I	22	Mx+	0.009	X	0.395	637	S	H	11			V	0.386
588	PS	H	23	(−)		X	0.395	638	APS	I	11	|M|	0.003	X	0.386
589	APS	I	22	|M|	0.006	X	0.395	639	TS	H	33	(−)		X	0.386
590	APS	I	23	|M|	0.005	X	0.394	640	APS	I	11	Res	0.002	X	0.385
591	APS	I	23	Mx−	0.005	X	0.394	641	APS	I	11	Mx+	0.002	X	0.385
592	APS	I	22	Mx+	0.007	X	0.394	642	PS	I	12	PV		V	0.385
593	APS	I	MxP	|M|	0.004	V	0.394	643	APS	I	23	|M|	0.001	V	0.385
594	APS	I	“M”		0.005	V	0.394	644	PS	I	22	|M|		X	0.385
595	APS	I	MxS		0.004	V	0.394	645	APS	I	23	|M|	0.0005	V	0.384
596	APS	I	MxP	Mx+	0.004	V	0.394	646	APS	I	23	Mx−	0.0005	V	0.384
597	APS	I	23	|M|	0.006	X	0.393	647	PSE	I	Shr			X	0.384
598	APS	I	23	Mx−	0.006	X	0.393	648	S	H	vM			V	0.384
599	APS	I	33	|M|	0.009	V	0.392	649	APS	I	23	Mx−	0.001	V	0.384
600	APS	I	23	Mx+	0.0005	X	0.392	650	TS	H	MnP			V	0.384
601	APS	I	“M”		0.04	V	0.392	651	APS	I	MxP	Mx−	0.007	V	0.383
602	M*A	I	22	|M|	0	X	0.392	652	APS	I	23	|M|	0.002	V	0.383
603	APS	I	22	Mx−	0.007	V	0.391	653	APS	I	23	Mx−	0.002	V	0.383
604	PS	I	MxP	|M|		V	0.391	654	S	H	MxS			V	0.383
605	PS	I	MxP	Mx+		V	0.391	655	S	H	Tca			V	0.383
606	TS	H	22	(−)		X	0.391	656	APS	I	11	|M|	0.002	X	0.382
607	S	H	prs			V	0.391	657	APS	I	33	Mx+	0.006	V	0.381
608	S	H	11	(−)		V	0.391	658	APS	I	23	|M|	0.003	V	0.381
609	APS	I	MnP	|M|	0.008	X	0.391	659	APS	I	23	Mx−	0.003	V	0.381
610	APS	I	MnP	Mx−	0.008	X	0.391	660	M*A	I	MxP	Mx−	0	V	0.381
611	APS	I	MxS		0.008	X	0.391	661	APS	I	13	Mx+	0.004	X	0.381
612	APS	I	11	Mx+	0.003	X	0.390	662	APS	I	22	|M|	0.008	V	0.381
613	APS	I	33	Mx+	0.007	V	0.390	663	APS	I	13	|M|	0.0005	X	0.380
614	APS	I	MxP	|M|	0.008	X	0.390	664	M*A	I	“E”		0	V	0.380
615	APS	I	MxP	Mx+	0.008	X	0.390	665	TS	H	MxS			V	0.380
616	TSE	H	Gnl			V	0.390	666	S	H	3rd	(−)		V	0.380
617	APS	I	22	Mx+	0.003	X	0.390	667	S	I	12	|M|		V	0.380
618	PS	H	33	(−)		V	0.390	668	APS	I	22	Mx+	0.001	X	0.379
619	S	H	MxP			V	0.390	669	APS	I	MnP	Mx+	0.007	V	0.379

Rank	Stm	TD	Cmp	Rgy	Thrsh	Mtl	Q	Rank	Stm	TD	Cmp	Rgy	Thrsh	Mtl	Q
620	APS	I	33	Mx+	0.009	V	0.389	670	S	I	13	Mx+		V	0.378
671	APS	I	12	|M|	0.005	X	0.378	721	APS	I	23	|M|	0.008	X	0.363
672	APS	I	12	Mx+	0.005	X	0.378	722	APS	I	23	Mx−	0.008	X	0.363
673	TSE	H	Nml			V	0.378	723	APS	I	22	Mx−	0.006	X	0.363
674	APS	I	13	|M|	0.002	V	0.378	724	APS	I	22	Mx+	0.01	X	0.362
675	APS	I	33	|M|	0.007	V	0.377	725	APS	I	11	|M|	0.004	X	0.361
676	S	I	12	Mx−		V	0.377	726	APS	I	33	Mx+	0.01	V	0.361
677	APS	I	13	Mx+	0.002	X	0.376	727	PS	I	11	PV		V	0.360
678	M*A	I	MnP	Mx+	0	V	0.376	728	M*A	I	12	|M|	0	X	0.360
679	APS	I	22	Mx−	0.002	V	0.376	729	M*A	I	12	Mx+	0	X	0.360
680	APS	I	“E”		0.01	X	0.376	730	APS	I	13	|M|	0.004	V	0.359
681	TS	H	23	(−)		X	0.376	731	APS	I	11	Mx+	0.004	X	0.358
682	PS	H	13	(+)		X	0.376	732	APS	I	22	Mx−	0.001	V	0.358
683	PSE	I	Shr			V	0.376	733	APS	I	22	Mx−	0.0005	V	0.358
684	PS	I	13	PV		X	0.375	734	APS	I	22	|M|	0.009	X	0.358
685	APS	I	22	Mx+	0.004	X	0.375	735	S	I	MnP	Mx+		V	0.358
686	M*A	I	11	Res	0	X	0.375	736	APS	I	22	Mx+	0.005	X	0.357
687	APS	I	22	Mx−	0.008	X	0.374	737	S	H	23	|m|		X	0.357
688	TS	H	MxP			V	0.373	738	S	I	12	|M|		X	0.357
689	TS	I	22	|M|		V	0.372	739	APS	I	“M”		0.02	V	0.357
690	M*A	I	11	Mx+	0	X	0.371	740	TS	H	MxP			X	0.357
691	S	H	23	(+)		X	0.371	741	APS	I	22	Mx+	0.0005	X	0.357
692	APS	I	12	|M|	0.009	X	0.371	742	APS	I	12	|M|	0.004	V	0.357
693	APS	I	12	Mx+	0.009	X	0.371	743	APS	I	12	Mx+	0.004	V	0.357
694	APS	I	MxP	Mx−	0.005	X	0.370	744	APS	I	“E”		0.08	X	0.356
695	APS	I	12	|M|	0.007	X	0.370	745	PS	H	23	(−)		V	0.356
696	APS	I	12	Mx+	0.007	X	0.370	746	APS	I	33	Mx−	0.008	V	0.356
697	S	H	23	(−)		X	0.369	747	M*A	I	23	Mx−	0	X	0.355
698	APS	I	13	Mx+	0.005	X	0.369	748	M*A	I	23	|M|	0	X	0.355
699	APS	I	33	|M|	0.006	V	0.368	749	TS	I	MnP	PV		V	0.355
700	PS	I	22	|M|		V	0.368	750	PS	H	11			X	0.355
701	PS	I	22	Mx+		V	0.368	751	APS	I	12	|M|	0.006	X	0.355
702	PS	H	33			V	0.368	752	APS	I	12	Mx+	0.006	X	0.355
703	APS	I	23	Mx+	0.01	V	0.368	753	TS	I	MxP	|M|		V	0.354
704	APS	I	13	Mx−	0.002	V	0.367	754	TS	I	MxP	Mx+		V	0.354
705	APS	I	“M”		0.009	X	0.367	755	APS	I	23	Mx+	0.001	X	0.354
706	APS	I	33	Mx−	0.005	V	0.367	756	TS	I	MxP	PV		V	0.354
707	APS	I	33	|M|	0.01	V	0.367	757	M*A	I	22	Mx−	0	X	0.354
708	APS	I	12	|M|	0.01	X	0.367	758	TS	I	MxS			V	0.354
709	APS	I	12	Mx+	0.01	X	0.367	759	TS	I	13	|M|		X	0.353
710	APS	I	12	|M|	0.004	X	0.367	760	TS	I	13	Mx+		X	0.353
711	APS	I	12	Mx+	0.004	X	0.367	761	S	I	13	|M|		X	0.353
712	S	H	22	(+)		V	0.367	762	APS	I	MxS		0.02	V	0.353
713	APS	I	12	|M|	0.008	X	0.366	763	TS	H	33	|m|		X	0.353
714	APS	I	12	Mx+	0.008	X	0.366	764	PS	H	13	|m|		X	0.352
715	TS	H	11	(+)		V	0.365	765	APS	I	12	|M|	0.002	X	0.352
716	TS	H	12			V	0.365	766	APS	I	12	Mx+	0.002	X	0.352
717	TS	I	MxS	PV		V	0.364	767	APS	I	23	|M|	0.01	X	0.352
718	APS	I	13	Mx−	0.0005	X	0.364	768	APS	I	23	Mx−	0.01	X	0.352
719	APS	I	23	|M|	0.007	X	0.363	769	APS	I	13	Mx+	0.0005	X	0.352
720	APS	I	23	Mx−	0.007	X	0.363	770	TS	I	13	|M|		V	0.352
771	TS	I	13	Mx+		V	0.352	821	APS	I	22	Mx−	0.01	X	0.345
772	S	H	23			V	0.351	822	PS	H	11	|m|		X	0.345
773	APS	I	23	|M|	0.009	X	0.351	823	PSE	H	Gnl			X	0.345
774	APS	I	23	Mx−	0.009	X	0.351	824	S	I	12	PV		V	0.345
775	APS	I	13	Mx+	0.001	V	0.351	825	APS	I	MxP	|M|	0.007	X	0.345

NIH-PA Author Manuscript
NIH-PA Author Manuscript

Rank	Stm	TD	Cmp	Rgy	Thrsh	Mtl	Q	Rank	Stm	TD	Cmp	Rgy	Thrsh	Mtl	Q
776	APS	I	22	|M|	0.01	X	0.351	826	APS	I	MxP	Mx+	0.007	X	0.345
777	APS	I	23	|M|	0.04	V	0.351	827	PS	I	11	Mx−		V	0.345
778	APS	I	23	Mx−	0.04	V	0.351	828	PS	H	12			X	0.344
779	APS	I	13	Mx+	0.004	V	0.351	829	PSE	H	Nml			X	0.344
780	APS	I	22	Mx−	0.002	X	0.351	830	TS	H	11			X	0.343
781	APS	I	12	|M|	0.003	X	0.350	831	S	H	13	|m|		X	0.343
782	APS	I	12	Mx+	0.003	X	0.350	832	TS	H	13	(+)		X	0.343
783	APS	I	13	Mx+	0.005	V	0.350	833	APS	I	11	Res	0.004	X	0.343
784	PS	I	12	Mx−		X	0.350	834	TS	H	MnP			X	0.343
785	S	H	Tca			X	0.349	835	TS	I	12	Mx−		V	0.342
786	S	H	MxS			X	0.349	836	M*A	I	11	|M|	0	X	0.342
787	TS	H	MxS			X	0.349	837	APS	I	33	Mx−	0.004	V	0.341
788	APS	I	22	Mx−	0.007	X	0.349	838	S	H	prs			X	0.341
789	S	H	vM			X	0.349	839	PS	H	33			X	0.340
790	TS	I	11	|M|		X	0.349	840	APS	I	22	Mx+	0.005	V	0.340
791	TS	I	11	Mx−		X	0.349	841	APS	I	13	Mx+	0.003	V	0.339
792	PS	H	"E"			X	0.349	842	TS	H	12	|m|		X	0.338
793	S	H	12	(−)		X	0.349	843	APS	I	MnP	Mx+	0.002	X	0.337
794	PS	H	12	|m|		X	0.349	844	APS	I	MxP	Mx−	0.002	X	0.337
795	APS	I	33	|M|	0.001	X	0.348	845	M*A	I	MnP	Mx+	0	X	0.337
796	PS	H	MnP			X	0.348	846	S	H	prs	(−)		V	0.336
797	PS	H	MxS			X	0.348	847	M*A	I	33	Mx−	0	V	0.336
798	PS	H	"M"			X	0.348	848	M*A	I	MxP	Mx−	0	X	0.336
799	TS	I	MnP	|M|		V	0.348	849	APS	I	23	|M|	0.06	V	0.335
800	TS	I	MnP	Mx−		V	0.348	850	APS	I	23	Mx−	0.06	V	0.335
801	APS	I	13	|M|	0.003	V	0.348	851	APS	I	13	Mx+	0.006	X	0.335
802	PS	H	22	|m|		X	0.348	852	S	I	13	Mx+		X	0.335
803	APS	I	22	Mx−	0.009	X	0.347	853	PS	H	23			X	0.335
804	TS	H	11	|m|		X	0.347	854	APS	I	"E"		0.009	X	0.334
805	APS	I	"E"		0.01	V	0.347	855	APS	I	13	|M|	0.006	V	0.334
806	PS	H	MxP			X	0.347	856	APS	I	"M"		0.01	V	0.334
807	APS	I	33	Mx+	0.001	X	0.347	857	APS	I	13	|M|	0.005	V	0.333
808	TS	H	11	(−)		X	0.347	858	S	H	13			X	0.333
809	APS	I	13	Mx+	0.006	V	0.347	859	APS	I	"M"		0.009	V	0.333
810	TS	I	MxP	Mx−		X	0.347	860	PS	H	23			V	0.333
811	PS	I	11	|M|		X	0.347	861	APS	I	MnP	Mx+	0.003	X	0.333
812	TSE	H	Shr			X	0.346	862	APS	I	MxP	Mx−	0.003	X	0.332
813	PSE	I	Gnl	PV		V	0.346	863	PS	H	33	|m|		X	0.332
814	APS	I	22	Mx−	0.001	X	0.346	864	APS	I	33	Mx−	0.007	V	0.332
815	APS	I	22	Mx−	0.0005	X	0.346	865	PS	H	23	|m|		X	0.332
816	APS	I	33	Mx−	0.003	V	0.346	866	PS	H	"E"			V	0.332
817	PS	I	11	|M|		V	0.346	867	PS	I	23	Mx+		X	0.331
818	PSE	H	Shr			X	0.346	868	APS	I	MnP	Mx+	0.004	X	0.331
819	S	I	13	Mx−		X	0.346	869	APS	I	11	Mx−	0.002	X	0.331
820	APS	I	22	Mx+	0.002	V	0.346	870	M*A	I	"M"		0	V	0.331
871	PS	I	12	|M|		X	0.331	921	APS	I	22	Mx+	0.01	V	0.320
872	PS	I	12	Mx+		X	0.331	922	S	H	prs	|m|		X	0.320
873	APS	I	13	Mx+	0.007	V	0.330	923	APS	I	33	|M|	0.002	X	0.319
874	TS	I	12	PV		V	0.330	924	APS	I	MxP	Mx−	0.006	X	0.319
875	APS	I	MxP	Mx−	0.004	X	0.330	925	APS	I	11	Mx−	0.005	X	0.319
876	APS	I	33	Mx−	0.009	V	0.330	926	S	H	12	|m|		X	0.319
877	TS	H	23	(+)		X	0.330	927	M*A	I	MxP	|M|	0	V	0.318
878	APS	I	11	Mx−	0.003	X	0.330	928	M*A	I	MxP	Mx+	0	V	0.318
879	S	H	3rd	|m|		X	0.330	929	APS	I	33	Mx−	0.006	V	0.318
880	S	I	MnP	Mx+		X	0.329	930	APS	I	13	|M|	0.005	X	0.317
881	PS	H	11	(−)		X	0.329	931	M*A	I	13	Mx+	0	X	0.317

Rank	Stm	TD	Cmp	Rgy	Thrsh	Mtl	Q	Rank	Stm	TD	Cmp	Rgy	Thrsh	Mtl	Q
882	PS	I	23	|M|		X	0.329	932	APS	I	MnP	Mx+	0.005	X	0.317
883	PS	I	23	Mx−		X	0.329	933	APS	I	11	|M|	0.005	X	0.317
884	PS	I	"E"			X	0.329	934	APS	I	MxP	|M|	0.01	V	0.315
885	TS	H	13	(+)		V	0.329	935	APS	I	MxP	Mx+	0.01	V	0.315
886	M*A	I	MxS		0	V	0.328	936	M*A	I	12	Mx−	0	X	0.315
887	M*A	I	MnP	|M|	0	V	0.328	937	APS	I	13	|M|	0.004	X	0.314
888	M*A	I	MnP	Mx−	0	V	0.328	938	APS	I	11	Mx−	0.004	X	0.314
889	APS	I	23	Mx+	0.01	X	0.328	939	APS	I	12	|M|	0.007	V	0.314
890	APS	I	MxP	|M|	0.008	V	0.327	940	APS	I	12	Mx+	0.007	V	0.314
891	APS	I	MxP	Mx+	0.008	V	0.327	941	APS	I	33	Mx−	0.0005	X	0.314
892	APS	I	MnP	|M|	0.008	V	0.327	942	PS	H	11	(+)		X	0.313
893	APS	I	MnP	Mx−	0.008	V	0.327	943	APS	I	23	|M|	0.02	X	0.313
894	APS	I	MxS		0.008	V	0.327	944	APS	I	23	Mx−	0.02	X	0.313
895	S	H	MnP			X	0.327	945	APS	I	MnP	Mx+	0.007	X	0.313
896	APS	I	12	|M|	0.03	X	0.327	946	S	H	12	(+)		V	0.313
897	APS	I	12	Mx+	0.03	X	0.327	947	TS	H	11	(+)		X	0.312
898	PS	I	11	Mx+		X	0.326	948	APS	I	23	|M|	0.03	X	0.312
899	TSE	H	Gnl			X	0.325	949	APS	I	23	Mx−	0.03	X	0.312
900	S	H	23			X	0.325	950	APS	I	MxS		0.01	V	0.312
901	APS	I	12	|M|	0.006	V	0.325	951	APS	I	13	Mx+	0.008	V	0.312
902	APS	I	12	Mx+	0.006	V	0.325	952	APS	I	MxP	Mx−	0.007	X	0.312
903	TS	I	22	Mx+		V	0.324	953	TS	H	12	(+)		V	0.311
904	S	H	13	(−)		X	0.324	954	M*A	I	23	Mx+	0	X	0.311
905	TS	I	11	Mx+		V	0.324	955	M*A	I	11	Mx−	0	X	0.311
906	APS	I	13	Mx−	0.003	V	0.324	956	M*A	I	12	Mx−	0	V	0.310
907	APS	I	22	|M|	0.007	V	0.323	957	S	H	13	(+)		X	0.310
908	PS	H	13			X	0.323	958	APS	I	11	Mx−	0.001	X	0.309
909	APS	I	12	|M|	0.02	X	0.323	959	APS	I	"E"		0.02	V	0.309
910	APS	I	12	Mx+	0.02	X	0.323	960	APS	I	12	|M|	0.04	X	0.308
911	APS	I	13	|M|	0.001	X	0.322	961	APS	I	12	Mx+	0.04	X	0.308
912	TS	H	12	(−)		X	0.322	962	TS	H	13			X	0.308
913	APS	I	MnP	Mx+	0.006	X	0.322	963	S	I	12	Mx+		V	0.308
914	TSE	H	Nml			X	0.322	964	APS	I	13	|M|	0.007	V	0.307
915	TS	H	33			X	0.322	965	PS	H	12			V	0.307
916	TS	H	22	|m|		X	0.321	966	APS	I	MxP	|M|	0.02	V	0.307
917	APS	I	12	|M|	0.005	V	0.321	967	APS	I	MxP	Mx+	0.02	V	0.307
918	APS	I	12	Mx+	0.005	V	0.321	968	TS	I	12	Mx−		X	0.306
919	APS	I	33	Mx+	0.002	X	0.321	969	APS	I	11	Mx−	0.0005	X	0.306
920	APS	I	12	Mx−	0.004	V	0.321	970	APS	I	"E"		0.07	V	0.305
971	APS	I	MnP	|M|	0.04	X	0.305	1021	APS	I	12	Mx−	0.002	X	0.292
972	APS	I	MnP	Mx−	0.04	X	0.305	1022	S	I	12	Mx−		X	0.292
973	APS	I	11	Mx−	0.006	X	0.305	1023	APS	I	33	Mx−	0.01	V	0.291
974	APS	I	11	Mx+	0.005	X	0.305	1024	APS	I	12	Mx−	0.007	X	0.291
975	APS	I	11	Res	0.005	X	0.305	1025	APS	I	11	Mx+	0.006	X	0.291
976	APS	I	MnP	Mx+	0.008	X	0.304	1026	APS	I	11	|M|	0.0005	X	0.291
977	S	I	11	Mx+		X	0.304	1027	APS	I	22	Mx+	0.009	V	0.290
978	APS	I	13	|M|	0.006	X	0.304	1028	APS	I	13	Mx+	0.007	X	0.289
979	APS	I	11	|M|	0.006	X	0.304	1029	APS	I	22	Mx+	0.004	V	0.289
980	TS	I	11	Mx+		X	0.303	1030	PS	I	33	Mx+		X	0.288
981	APS	I	13	Mx−	0.004	V	0.302	1031	PS	I	22	Mx−		X	0.288
982	APS	I	13	|M|	0.002	X	0.302	1032	APS	I	11	Res	0.0005	X	0.288
983	TS	I	12	|M|		V	0.302	1033	APS	I	33	Mx+	0.003	X	0.287
984	TS	I	12	Mx+		V	0.302	1034	APS	I	12	|M|	0.01	V	0.287
985	APS	I	33	Mx−	0.001	X	0.301	1035	APS	I	12	Mx+	0.01	V	0.287
986	PS	I	11	Mx−		X	0.301	1036	APS	I	MxS		0.009	V	0.287
987	APS	I	12	Mx−	0.006	X	0.300	1037	APS	I	11	|M|	0.008	X	0.287

Rank	Stm	TD	Cmp	Rgy	Thrsh	Mtl	Q	Rank	Stm	TD	Cmp	Rgy	Thrsh	Mtl	Q
988	PSE	H	Shr			V	0.300	1038	APS	I	11	Mx−	0.008	X	0.287
989	APS	I	12	|M|	0.008	V	0.300	1039	APS	I	33	|M|	0.003	X	0.286
990	APS	I	12	Mx+	0.008	V	0.300	1040	M*A	I	13	|M|	0	V	0.286
991	APS	I	23	Mx+	0.02	X	0.299	1041	APS	I	12	|M|	0.05	X	0.286
992	APS	I	23	|M|	0.04	X	0.299	1042	APS	I	12	Mx+	0.05	X	0.286
993	APS	I	23	Mx−	0.04	X	0.299	1043	APS	I	12	|M|	0.009	V	0.285
994	S	H	3rd			V	0.298	1044	APS	I	12	Mx+	0.009	V	0.285
995	APS	I	MnP	Mx+	0.009	X	0.298	1045	TS	H	23			X	0.285
996	APS	I	MnP	|M|	0.01	V	0.298	1046	PS	H	12	(−)		X	0.284
997	APS	I	MnP	Mx−	0.01	V	0.298	1047	APS	I	MnP	|M|	0.009	V	0.283
998	PS	H	13			V	0.298	1048	APS	I	MnP	Mx−	0.009	V	0.283
999	APS	I	13	Mx−	0.001	X	0.296	1049	TS	I	11	PV		V	0.282
1000	TS	H	22	(+)		V	0.296	1050	PS	I	13	|M|		X	0.282
1001	M*A	I	13	Mx−	0	V	0.296	1051	PS	I	13	Mx+		X	0.282
1002	PSE	I	Nml	PV		V	0.296	1052	APS	I	MxP	|M|	0.03	V	0.281
1003	APS	I	33	Mx−	0.003	X	0.296	1053	APS	I	MxP	Mx+	0.03	V	0.281
1004	M*A	I	13	|M|	0	X	0.295	1054	S	H	22	|m|		X	0.281
1005	APS	I	13	|M|	0.008	V	0.295	1055	TS	H	13			V	0.280
1006	S	H	11			X	0.294	1056	APS	I	22	|M|	0.004	X	0.279
1007	TS	H	22			X	0.294	1057	APS	I	13	Mx+	0.009	V	0.279
1008	S	H	22			X	0.294	1058	M*A	I	13	Mx+	0	V	0.278
1009	APS	I	11	|M|	0.007	X	0.294	1059	S	H	3rd			X	0.278
1010	APS	I	11	Mx−	0.007	X	0.294	1060	APS	I	13	Mx−	0.005	V	0.278
1011	S	H	33			X	0.293	1061	APS	I	22	Mx−	0.004	X	0.278
1012	PS	H	13	(+)		V	0.293	1062	PS	H	12	(+)		V	0.278
1013	APS	I	23	Mx+	0.002	X	0.293	1063	APS	I	13	|M|	0.009	V	0.278
1014	APS	I	MxP	|M|	0.009	V	0.293	1064	S	H	MxP			X	0.277
1015	APS	I	MxP	Mx+	0.009	V	0.293	1065	APS	I	11	Res	0.006	X	0.276
1016	PSE	I	Gnl			V	0.293	1066	PS	H	"M"			V	0.276
1017	APS	I	MnP	|M|	0.005	V	0.292	1067	PS	I	11	Mx+		V	0.276
1018	APS	I	MnP	Mx−	0.005	V	0.292	1068	PS	H	MnP			V	0.276
1019	APS	I	MxP	Mx−	0.008	X	0.292	1069	PSE	I	Nml			V	0.275
1020	APS	I	13	|M|	0.003	X	0.292	1070	APS	I	11	Mx+	0.0005	X	0.275
1071	APS	I	13	|M|	0.01	V	0.275	1121	PS	H	22	(+)		V	0.255
1072	APS	I	13	Mx+	0.01	V	0.275	1122	APS	I	11	Mx−	0.0005	V	0.255
1073	APS	I	12	Mx−	0.005	X	0.274	1123	TS	H	12	|m|		V	0.255
1074	PSE	H	Gnl			V	0.274	1124	M*A	I	33	Mx+	0	X	0.255
1075	APS	I	13	|M|	0.007	X	0.273	1125	S	H	11	(+)		V	0.254
1076	APS	I	11	|M|	0.01	X	0.273	1126	PS	H	13	|m|		V	0.254
1077	APS	I	11	Mx−	0.01	X	0.273	1127	APS	I	12	|M|	0.06	X	0.253
1078	PS	H	MxS			V	0.272	1128	APS	I	12	Mx+	0.06	X	0.253
1079	PS	H	22	|m|		V	0.272	1129	S	H	11	|m|		X	0.253
1080	APS	I	13	Mx+	0.008	X	0.271	1130	APS	I	11	Mx+	0.008	X	0.251
1081	APS	I	12	Mx−	0.004	X	0.271	1131	APS	I	23	Mx+	0.008	X	0.251
1082	S	H	33	|m|		X	0.271	1132	M*A	I	33	Mx−	0	X	0.251
1083	APS	I	11	Mx+	0.007	X	0.270	1133	APS	I	11	|M|	0.002	V	0.250
1084	APS	I	22	Mx+	0.008	V	0.270	1134	APS	I	11	Res	0.002	V	0.250
1085	APS	I	11	|M|	0.009	X	0.270	1135	APS	I	11	Mx+	0.003	V	0.250
1086	APS	I	11	Mx−	0.009	X	0.270	1136	APS	I	33	Mx−	0.006	X	0.249
1087	APS	I	22	Mx+	0.006	V	0.270	1137	APS	I	11	Res	0.008	X	0.247
1088	APS	I	11	Res	0.007	X	0.270	1138	APS	I	23	Mx+	0.005	X	0.245
1089	S	H	prs	|m|		V	0.270	1139	APS	I	13	Mx−	0.006	V	0.245
1090	S	H	12	|m|		V	0.269	1140	TS	H	33	(+)		X	0.245
1091	PS	H	MxP			V	0.269	1141	APS	I	13	Mx−	0.002	X	0.245
1092	APS	I	13	|M|	0.01	X	0.267	1142	TS	H	23	|m|		V	0.244
1093	APS	I	13	Mx+	0.01	X	0.267	1143	APS	I	23	|M|	0.05	X	0.244

Rank	Stm	TD	Cmp	Rgy	Thrsh	Mtl	Q	Rank	Stm	TD	Cmp	Rgy	Thrsh	Mtl	Q
1094	APS	I	12	Mx−	0.005	V	0.267	1144	APS	I	23	Mx−	0.05	X	0.244
1095	M*A	I	22	Mx+	0	V	0.266	1145	APS	I	11	|M|	0.003	V	0.244
1096	APS	I	13	|M|	0.008	X	0.266	1146	S	H	3rd	|m|		V	0.240
1097	APS	I	23	Mx+	0.003	X	0.266	1147	APS	I	11	Res	0.003	V	0.240
1098	APS	I	13	Mx+	0.009	X	0.266	1148	M*A	I	12	|M|	0	V	0.240
1099	APS	I	22	Mx+	0.003	V	0.266	1149	M*A	I	12	Mx+	0	V	0.240
1100	APS	I	33	|M|	0.005	X	0.265	1150	APS	I	12	Mx−	0.008	X	0.240
1101	APS	I	13	|M|	0.009	X	0.264	1151	APS	I	23	Mx+	0.006	X	0.237
1102	APS	I	33	Mx−	0.002	X	0.264	1152	S	H	23	|m|		V	0.237
1103	M*A	I	33	|M|	0	X	0.263	1153	APS	I	12	Mx−	0.003	X	0.237
1104	APS	I	23	Mx+	0.004	X	0.263	1154	PS	H	12	|m|		V	0.237
1105	APS	I	11	Mx+	0.001	V	0.262	1155	APS	I	33	Mx−	0.007	X	0.237
1106	APS	I	23	Mx+	0.009	X	0.262	1156	PS	H	33	|m|		V	0.236
1107	TS	H	13	|m|		V	0.262	1157	APS	I	22	Mx+	0.02	X	0.236
1108	APS	I	11	Res	0.001	V	0.261	1158	APS	I	12	|M|	0.02	V	0.236
1109	APS	I	11	|M|	0.001	V	0.261	1159	APS	I	12	Mx+	0.02	V	0.236
1110	APS	I	MxP	Mx−	0.008	V	0.260	1160	APS	I	12	Mx−	0.009	X	0.234
1111	PS	H	22			V	0.259	1161	APS	I	12	Mx−	0.006	V	0.233
1112	APS	I	33	Mx+	0.005	X	0.259	1162	APS	I	23	Mx+	0.007	X	0.232
1113	PSE	H	Nml			V	0.259	1163	TS	I	11	|M|		V	0.231
1114	APS	I	22	Mx+	0.007	V	0.259	1164	TS	I	11	Mx−		V	0.231
1115	APS	I	22	|M|	0.02	V	0.258	1165	PS	I	22	PV		V	0.228
1116	PS	H	23	(+)		X	0.258	1166	M*A	I	13	Mx−	0	X	0.227
1117	APS	I	33	|M|	0.004	X	0.258	1167	M*A	I	11	Res	0	V	0.227
1118	APS	I	33	Mx+	0.004	X	0.256	1168	PS	H	23	|m|		V	0.226
1119	APS	I	MnP	Mx+	0.008	V	0.256	1169	TS	H	11	(−)		V	0.226
1120	APS	I	11	Mx+	0.002	V	0.255	1170	M*A	I	11	Mx+	0	V	0.225
1171	APS	I	12	Mx−	0.01	X	0.224	1221	APS	I	33	Mx+	0.01	X	0.188
1172	APS	I	33	Mx−	0.005	X	0.224	1222	PS	H	11	(−)		V	0.187
1173	APS	I	33	|M|	0.007	X	0.224	1223	APS	I	12	Mx−	0.008	V	0.187
1174	PS	H	11	|m|		V	0.223	1224	APS	I	11	Mx−	0.003	V	0.186
1175	TS	H	11	|m|		V	0.223	1225	S	H	11	|m|		V	0.185
1176	APS	I	23	|M|	0.06	X	0.223	1226	APS	I	12	|M|	0.03	V	0.183
1177	APS	I	23	Mx−	0.06	X	0.223	1227	APS	I	12	Mx+	0.03	V	0.183
1178	TS	H	11			V	0.223	1228	APS	I	12	Mx−	0.01	V	0.182
1179	S	H	12	(−)		V	0.222	1229	APS	I	33	Mx−	0.01	X	0.181
1180	TS	H	23			V	0.222	1230	APS	I	11	Mx−	0.004	V	0.181
1181	APS	I	11	Mx−	0.001	V	0.222	1231	APS	I	33	Mx−	0.009	X	0.179
1182	APS	I	33	|M|	0.006	X	0.222	1232	APS	I	11	Res	0.004	V	0.178
1183	APS	I	MxP	Mx−	0.009	X	0.222	1233	M*A	I	11	Mx−	0	V	0.177
1184	APS	I	13	Mx−	0.003	X	0.221	1234	APS	I	12	Mx−	0.009	V	0.173
1185	TS	H	33	|m|		V	0.221	1235	APS	I	11	Mx−	0.005	V	0.172
1186	APS	I	33	|M|	0.008	X	0.219	1236	APS	I	11	Res	0.009	X	0.170
1187	PS	I	12	Mx−		V	0.219	1237	APS	I	11	|M|	0.005	V	0.170
1188	TS	H	13	(−)		X	0.217	1238	APS	I	13	Mx−	0.007	X	0.170
1189	APS	I	33	Mx+	0.007	X	0.217	1239	APS	I	12	|M|	0.04	V	0.168
1190	APS	I	33	Mx−	0.008	X	0.215	1240	APS	I	12	Mx+	0.04	V	0.168
1191	APS	I	MxP	Mx−	0.01	X	0.215	1241	APS	I	12	|M|	0.07	X	0.167
1192	APS	I	MnP	Mx+	0.01	X	0.215	1242	APS	I	12	Mx+	0.07	X	0.167
1193	TS	I	MnP	Mx+		X	0.214	1243	PS	I	13	Mx−		X	0.162
1194	S	H	33	|m|		V	0.213	1244	APS	I	11	Mx+	0.005	V	0.159
1195	APS	I	33	Mx+	0.006	X	0.213	1245	APS	I	11	Res	0.005	V	0.159
1196	TS	H	22	|m|		V	0.212	1246	PS	H	11	(+)		V	0.159
1197	S	H	22	|m|		V	0.209	1247	APS	I	11	Mx−	0.006	V	0.159
1198	APS	I	22	Mx−	0.02	X	0.209	1248	APS	I	11	|M|	0.006	V	0.158
1199	APS	I	33	Mx+	0.008	X	0.209	1249	TS	I	MxP	Mx−		V	0.154

Rank	Stm	TD	Cmp	Rgy	Thrsh	Mtl	Q	Rank	Stm	TD	Cmp	Rgy	Thrsh	Mtl	Q
1200	S	H	13			V	0.208	1250	PS	H	33	(+)		X	0.154
1201	TS	H	22			V	0.207	1251	APS	I	11	|M|	0.02	X	0.151
1202	PS	H	11			V	0.206	1252	APS	I	11	Mx−	0.02	X	0.151
1203	APS	I	33	|M|	0.009	X	0.206	1253	APS	I	11	|M|	0.008	V	0.150
1204	APS	I	11	Mx+	0.009	X	0.204	1254	APS	I	11	Mx−	0.008	V	0.150
1205	PS	H	12	(−)		V	0.203	1255	APS	I	13	|M|	0.02	X	0.150
1206	APS	I	11	|M|	0.004	V	0.203	1256	APS	I	13	Mx+	0.02	X	0.150
1207	TS	H	12	(−)		V	0.202	1257	APS	I	13	Mx−	0.008	V	0.150
1208	APS	I	12	Mx−	0.007	V	0.202	1258	APS	I	11	|M|	0.02	V	0.149
1209	M*A	I	11	|M|	0	V	0.201	1259	APS	I	11	Mx−	0.02	V	0.149
1210	APS	I	11	Mx+	0.004	V	0.200	1260	PS	H	33	(+)		V	0.149
1211	S	H	13	|m|		V	0.200	1261	APS	I	11	|M|	0.007	V	0.148
1212	APS	I	33	Mx−	0.004	X	0.199	1262	APS	I	11	Mx−	0.007	V	0.148
1213	APS	I	33	Mx+	0.009	X	0.199	1263	APS	I	11	Mx+	0.006	V	0.148
1214	APS	I	22	Mx−	0.02	V	0.198	1264	APS	I	13	Mx−	0.009	X	0.147
1215	APS	I	13	Mx−	0.007	V	0.196	1265	APS	I	13	Mx−	0.01	X	0.147
1216	APS	I	11	Mx−	0.002	V	0.196	1266	APS	I	13	Mx−	0.008	X	0.145
1217	APS	I	33	|M|	0.01	X	0.191	1267	APS	I	MnP	Mx+	0.009	V	0.144
1218	APS	I	13	Mx−	0.005	X	0.190	1268	APS	I	12	|M|	0.05	V	0.142
1219	APS	I	13	Mx−	0.004	X	0.190	1269	APS	I	12	Mx+	0.05	V	0.142
1220	APS	I	13	Mx−	0.006	X	0.189	1270	APS	I	MxP	Mx−	0.009	V	0.139
1271	APS	I	MxS		0.04	X	0.138	1321	APS	I	“E”	Res	0.02	V	0.059
1272	APS	I	11	Res	0.007	V	0.138	1322	APS	I	MxS	Res	0.02	V	0.059
1273	APS	I	11	Mx+	0.007	V	0.137	1323	APS	I	MnP	Res	0.02	V	0.059
1274	APS	I	11	|M|	0.009	V	0.136	1324	APS	I	MxP	Res	0.02	V	0.059
1275	APS	I	11	Mx−	0.009	V	0.136	1325	APS	I	33	Res	0.02	V	0.059
1276	APS	I	13	Mx−	0.009	V	0.135	1326	APS	I	22	Res	0.02	V	0.059
1277	APS	I	11	Mx+	0.009	V	0.135	1327	APS	I	“M”	Res	0.01	V	0.059
1278	APS	I	11	Res	0.006	V	0.135	1328	APS	I	“E”	Res	0.01	V	0.059
1279	APS	I	11	Mx+	0.008	V	0.134	1329	APS	I	MxS	Res	0.01	V	0.059
1280	PS	I	33	Mx+		V	0.132	1330	APS	I	23	Res	0.01	V	0.059
1281	APS	I	11	|M|	0.01	V	0.132	1331	APS	I	MnP	Res	0.01	V	0.059
1282	APS	I	11	Mx−	0.01	V	0.132	1332	APS	I	MxP	Res	0.01	V	0.059
1283	APS	I	12	|M|	0.06	V	0.130	1333	APS	I	33	Res	0.01	V	0.059
1284	APS	I	12	Mx+	0.06	V	0.130	1334	APS	I	22	Res	0.01	V	0.059
1285	APS	I	22	Mx+	0.02	V	0.127	1335	APS	I	“M”	Res	0.009	V	0.059
1286	APS	I	11	Res	0.008	V	0.121	1336	APS	I	“E”	Res	0.009	V	0.059
1287	PS	I	MnP	Mx+		X	0.120	1337	APS	I	MxS	Res	0.009	V	0.059
1288	PS	I	MxP	Mx−		X	0.120	1338	APS	I	23	Res	0.009	V	0.059
1289	APS	I	12	|M|	0.07	V	0.118	1339	APS	I	MnP	Res	0.009	V	0.059
1290	APS	I	12	Mx+	0.07	V	0.118	1340	APS	I	MxP	Res	0.009	V	0.059
1291	APS	I	11	Mx+	0.01	V	0.117	1341	APS	I	33	Res	0.009	V	0.059
1292	PS	I	13	Mx−		V	0.117	1342	APS	I	22	Res	0.009	V	0.059
1293	PS	I	MxP	Mx−		V	0.117	1343	APS	I	“M”	Res	0.008	V	0.059
1294	PS	I	22	Mx−		V	0.117	1344	APS	I	“E”	Res	0.008	V	0.059
1295	PS	I	MnP	Mx+		V	0.117	1345	APS	I	MxS	Res	0.008	V	0.059
1296	APS	I	13	|M|	0.02	V	0.115	1346	APS	I	23	Res	0.008	V	0.059
1297	APS	I	13	Mx+	0.02	V	0.115	1347	APS	I	MnP	Res	0.008	V	0.059
1298	APS	I	11	Res	0.009	V	0.114	1348	APS	I	MxP	Res	0.008	V	0.059
1299	APS	I	11	Mx+	0.01	X	0.112	1349	APS	I	33	Res	0.008	V	0.059
1300	APS	I	MnP	Mx+	0.01	V	0.111	1350	APS	I	22	Res	0.008	V	0.059
1301	APS	I	13	Mx−	0.01	V	0.109	1351	APS	I	“M”	Res	0.007	V	0.059
1302	APS	I	MxP	Mx−	0.01	V	0.106	1352	APS	I	“E”	Res	0.007	V	0.059
1303	TS	I	MnP	Mx+		V	0.100	1353	APS	I	MxS	Res	0.007	V	0.059
1304	APS	I	MnP	|M|	0.04	V	0.099	1354	APS	I	23	Res	0.007	V	0.059
1305	APS	I	MnP	Mx−	0.04	V	0.099	1355	APS	I	MnP	Res	0.007	V	0.059

NIH-PA Author Manuscript
NIH-PA Author Manuscript

Rank	Stm	TD	Cmp	Rgy	Thrsh	Mtl	Q	Rank	Stm	TD	Cmp	Rgy	Thrsh	Mtl	Q
1306	APS	I	MxS		0.04	V	0.095	1356	APS	I	MxP	Res	0.007	V	0.059
1307	APS	I	“E”		0.08	V	0.085	1357	APS	I	33	Res	0.007	V	0.059
1308	M*A	I	“M”	Res	0	V	0.059	1358	APS	I	22	Res	0.007	V	0.059
1309	M*A	I	“E”	Res	0	V	0.059	1359	APS	I	“M”	Res	0.006	V	0.059
1310	M*A	I	MxS	Res	0	V	0.059	1360	APS	I	“E”	Res	0.006	V	0.059
1311	M*A	I	23	Res	0	V	0.059	1361	APS	I	MxS	Res	0.006	V	0.059
1312	M*A	I	13	Res	0	V	0.059	1362	APS	I	23	Res	0.006	V	0.059
1313	M*A	I	12	Res	0	V	0.059	1363	APS	I	MnP	Res	0.006	V	0.059
1314	M*A	I	MnP	Res	0	V	0.059	1364	APS	I	MxP	Res	0.006	V	0.059
1315	M*A	I	MxP	Res	0	V	0.059	1365	APS	I	33	Res	0.006	V	0.059
1316	M*A	I	33	Res	0	V	0.059	1366	APS	I	22	Res	0.006	V	0.059
1317	M*A	I	22	Res	0	V	0.059	1367	APS	I	“M”	Res	0.005	V	0.059
1318	APS	I	“M”	Res	0.03	V	0.059	1368	APS	I	“E”	Res	0.005	V	0.059
1319	APS	I	“E”	Res	0.03	V	0.059	1369	APS	I	MxS	Res	0.005	V	0.059
1320	APS	I	“M”	Res	0.02	V	0.059	1370	APS	I	23	Res	0.005	V	0.059
1371	APS	I	MnP	Res	0.005	V	0.059	1421	APS	I	23	Mx−	0.07	V	0.048
1372	APS	I	MxP	Res	0.005	V	0.059	1422	APS	I	23	Mx+	0.02	V	0.046
1373	APS	I	33	Res	0.005	V	0.059	1423	M*A	I	“M”	Res	0	X	0.035
1374	APS	I	22	Res	0.005	V	0.059	1424	M*A	I	“E”	Res	0	X	0.035
1375	APS	I	“M”	Res	0.004	V	0.059	1425	M*A	I	MxS	Res	0	X	0.035
1376	APS	I	“E”	Res	0.004	V	0.059	1426	M*A	I	23	Res	0	X	0.035
1377	APS	I	MxS	Res	0.004	V	0.059	1427	M*A	I	13	Res	0	X	0.035
1378	APS	I	23	Res	0.004	V	0.059	1428	M*A	I	12	Res	0	X	0.035
1379	APS	I	MnP	Res	0.004	V	0.059	1429	M*A	I	MnP	Res	0	X	0.035
1380	APS	I	MxP	Res	0.004	V	0.059	1430	M*A	I	MxP	Res	0	X	0.035
1381	APS	I	33	Res	0.004	V	0.059	1431	M*A	I	33	Res	0	X	0.035
1382	APS	I	22	Res	0.004	V	0.059	1432	M*A	I	22	Res	0	X	0.035
1383	APS	I	“M”	Res	0.003	V	0.059	1433	APS	I	“M”	Res	0.03	X	0.035
1384	APS	I	“E”	Res	0.003	V	0.059	1434	APS	I	“E”	Res	0.03	X	0.035
1385	APS	I	MxS	Res	0.003	V	0.059	1435	APS	I	“M”	Res	0.02	X	0.035
1386	APS	I	23	Res	0.003	V	0.059	1436	APS	I	“E”	Res	0.02	X	0.035
1387	APS	I	MnP	Res	0.003	V	0.059	1437	APS	I	MxS	Res	0.02	X	0.035
1388	APS	I	MxP	Res	0.003	V	0.059	1438	APS	I	MnP	Res	0.02	X	0.035
1389	APS	I	33	Res	0.003	V	0.059	1439	APS	I	MxP	Res	0.02	X	0.035
1390	APS	I	22	Res	0.003	V	0.059	1440	APS	I	33	Res	0.02	X	0.035
1391	APS	I	“M”	Res	0.002	V	0.059	1441	APS	I	22	Res	0.02	X	0.035
1392	APS	I	“E”	Res	0.002	V	0.059	1442	APS	I	“M”	Res	0.01	X	0.035
1393	APS	I	MxS	Res	0.002	V	0.059	1443	APS	I	“E”	Res	0.01	X	0.035
1394	APS	I	23	Res	0.002	V	0.059	1444	APS	I	MxS	Res	0.01	X	0.035
1395	APS	I	MnP	Res	0.002	V	0.059	1445	APS	I	23	Res	0.01	X	0.035
1396	APS	I	MxP	Res	0.002	V	0.059	1446	APS	I	MnP	Res	0.01	X	0.035
1397	APS	I	33	Res	0.002	V	0.059	1447	APS	I	MxP	Res	0.01	X	0.035
1398	APS	I	22	Res	0.002	V	0.059	1448	APS	I	33	Res	0.01	X	0.035
1399	APS	I	“M”	Res	0.001	V	0.059	1449	APS	I	22	Res	0.01	X	0.035
1400	APS	I	“E”	Res	0.001	V	0.059	1450	APS	I	“M”	Res	0.009	X	0.035
1401	APS	I	MxS	Res	0.001	V	0.059	1451	APS	I	“E”	Res	0.009	X	0.035
1402	APS	I	23	Res	0.001	V	0.059	1452	APS	I	MxS	Res	0.009	X	0.035
1403	APS	I	MnP	Res	0.001	V	0.059	1453	APS	I	23	Res	0.009	X	0.035
1404	APS	I	MxP	Res	0.001	V	0.059	1454	APS	I	MnP	Res	0.009	X	0.035
1405	APS	I	33	Res	0.001	V	0.059	1455	APS	I	MxP	Res	0.009	X	0.035
1406	APS	I	22	Res	0.001	V	0.059	1456	APS	I	33	Res	0.009	X	0.035
1407	APS	I	“M”	Res	0.0005	V	0.059	1457	APS	I	22	Res	0.009	X	0.035
1408	APS	I	“E”	Res	0.0005	V	0.059	1458	APS	I	“M”	Res	0.008	X	0.035
1409	APS	I	MxS	Res	0.0005	V	0.059	1459	APS	I	“E”	Res	0.008	X	0.035
1410	APS	I	23	Res	0.0005	V	0.059	1460	APS	I	MxS	Res	0.008	X	0.035
1411	APS	I	MnP	Res	0.0005	V	0.059	1461	APS	I	23	Res	0.008	X	0.035

NIH-PA Author Manuscript
NIH-PA Author Manuscript

Rank	Stm	TD	Cmp	Rgy	Thrsh	Mtl	Q	Rank	Stm	TD	Cmp	Rgy	Thrsh	Mtl	Q
1412	APS	I	MxP	Res	0.0005	V	0.059	1462	APS	I	MnP	Res	0.008	X	0.035
1413	APS	I	33	Res	0.0005	V	0.059	1463	APS	I	MxP	Res	0.008	X	0.035
1414	APS	I	22	Res	0.0005	V	0.059	1464	APS	I	33	Res	0.008	X	0.035
1415	APS	I	33	|M|	0.02	V	0.059	1465	APS	I	22	Res	0.008	X	0.035
1416	APS	I	MxP	Mx−	0.02	V	0.059	1466	APS	I	“M”	Res	0.007	X	0.035
1417	APS	I	33	Mx−	0.02	V	0.059	1467	APS	I	“E”	Res	0.007	X	0.035
1418	APS	I	MnP	Mx+	0.02	V	0.059	1468	APS	I	MxS	Res	0.007	X	0.035
1419	APS	I	33	Mx+	0.02	V	0.059	1469	APS	I	23	Res	0.007	X	0.035
1420	APS	I	23	|M|	0.07	V	0.048	1470	APS	I	MnP	Res	0.007	X	0.035
1471	APS	I	MxP	Res	0.007	X	0.035	1521	APS	I	22	Res	0.001	X	0.035
1472	APS	I	33	Res	0.007	X	0.035	1522	APS	I	“M”	Res	0.0005	X	0.035
1473	APS	I	22	Res	0.007	X	0.035	1523	APS	I	“E”	Res	0.0005	X	0.035
1474	APS	I	“M”	Res	0.006	X	0.035	1524	APS	I	MxS	Res	0.0005	X	0.035
1475	APS	I	“E”	Res	0.006	X	0.035	1525	APS	I	23	Res	0.0005	X	0.035
1476	APS	I	MxS	Res	0.006	X	0.035	1526	APS	I	MnP	Res	0.0005	X	0.035
1477	APS	I	23	Res	0.006	X	0.035	1527	APS	I	MxP	Res	0.0005	X	0.035
1478	APS	I	MnP	Res	0.006	X	0.035	1528	APS	I	33	Res	0.0005	X	0.035
1479	APS	I	MxP	Res	0.006	X	0.035	1529	APS	I	22	Res	0.0005	X	0.035
1480	APS	I	33	Res	0.006	X	0.035	1530	APS	I	33	|M|	0.02	X	0.035
1481	APS	I	22	Res	0.006	X	0.035	1531	APS	I	MxP	Mx−	0.02	X	0.035
1482	APS	I	“M”	Res	0.005	X	0.035	1532	APS	I	33	Mx−	0.02	X	0.035
1483	APS	I	“E”	Res	0.005	X	0.035	1533	APS	I	MnP	Mx+	0.02	X	0.035
1484	APS	I	MxS	Res	0.005	X	0.035	1534	APS	I	33	Mx+	0.02	X	0.035
1485	APS	I	23	Res	0.005	X	0.035	1535	PS	H	22	(−)		V	NaN
1486	APS	I	MnP	Res	0.005	X	0.035	1536	PS	H	13	(−)		V	NaN
1487	APS	I	MxP	Res	0.005	X	0.035	1537	APS	I	11	Mx+	0.02	V	NaN
1488	APS	I	33	Res	0.005	X	0.035	1538	APS	I	11	Mx+	0.03	V	NaN
1489	APS	I	22	Res	0.005	X	0.035	1539	APS	I	22	Mx+	0.03	V	NaN
1490	APS	I	“M”	Res	0.004	X	0.035	1540	APS	I	33	Mx+	0.03	V	NaN
1491	APS	I	“E”	Res	0.004	X	0.035	1541	APS	I	MnP	Mx+	0.03	V	NaN
1492	APS	I	MxS	Res	0.004	X	0.035	1542	APS	I	13	Mx+	0.03	V	NaN
1493	APS	I	23	Res	0.004	X	0.035	1543	APS	I	23	Mx+	0.03	V	NaN
1494	APS	I	MnP	Res	0.004	X	0.035	1544	APS	I	11	Mx+	0.04	V	NaN
1495	APS	I	MxP	Res	0.004	X	0.035	1545	APS	I	22	Mx+	0.04	V	NaN
1496	APS	I	33	Res	0.004	X	0.035	1546	APS	I	33	Mx+	0.04	V	NaN
1497	APS	I	22	Res	0.004	X	0.035	1547	APS	I	MxP	Mx+	0.04	V	NaN
1498	APS	I	“M”	Res	0.003	X	0.035	1548	APS	I	MnP	Mx+	0.04	V	NaN
1499	APS	I	“E”	Res	0.003	X	0.035	1549	APS	I	13	Mx+	0.04	V	NaN
1500	APS	I	MxS	Res	0.003	X	0.035	1550	APS	I	23	Mx+	0.04	V	NaN
1501	APS	I	23	Res	0.003	X	0.035	1551	APS	I	11	Mx+	0.05	V	NaN
1502	APS	I	MnP	Res	0.003	X	0.035	1552	APS	I	22	Mx+	0.05	V	NaN
1503	APS	I	MxP	Res	0.003	X	0.035	1553	APS	I	33	Mx+	0.05	V	NaN
1504	APS	I	33	Res	0.003	X	0.035	1554	APS	I	MxP	Mx+	0.05	V	NaN
1505	APS	I	22	Res	0.003	X	0.035	1555	APS	I	MnP	Mx+	0.05	V	NaN
1506	APS	I	“M”	Res	0.002	X	0.035	1556	APS	I	13	Mx+	0.05	V	NaN
1507	APS	I	“E”	Res	0.002	X	0.035	1557	APS	I	23	Mx+	0.05	V	NaN
1508	APS	I	MxS	Res	0.002	X	0.035	1558	APS	I	MxS		0.05	V	NaN
1509	APS	I	23	Res	0.002	X	0.035	1559	APS	I	“M”		0.05	V	NaN
1510	APS	I	MnP	Res	0.002	X	0.035	1560	APS	I	11	Mx+	0.06	V	NaN
1511	APS	I	MxP	Res	0.002	X	0.035	1561	APS	I	22	Mx+	0.06	V	NaN
1512	APS	I	33	Res	0.002	X	0.035	1562	APS	I	33	Mx+	0.06	V	NaN
1513	APS	I	22	Res	0.002	X	0.035	1563	APS	I	MxP	Mx+	0.06	V	NaN
1514	APS	I	“M”	Res	0.001	X	0.035	1564	APS	I	MnP	Mx+	0.06	V	NaN
1515	APS	I	“E”	Res	0.001	X	0.035	1565	APS	I	13	Mx+	0.06	V	NaN
1516	APS	I	MxS	Res	0.001	X	0.035	1566	APS	I	23	Mx+	0.06	V	NaN
1517	APS	I	23	Res	0.001	X	0.035	1567	APS	I	MxS		0.06	V	NaN

Rank	Stm	TD	Cmp	Rgy	Thrsh	Mtl	Q	Rank	Stm	TD	Cmp	Rgy	Thrsh	Mtl	Q
1518	APS	I	MnP	Res	0.001	X	0.035	1568	APS	I	"M"		0.06	V	NaN
1519	APS	I	MxP	Res	0.001	X	0.035	1569	APS	I	11	Mx+	0.07	V	NaN
1520	APS	I	33	Res	0.001	X	0.035	1570	APS	I	22	Mx+	0.07	V	NaN
1571	APS	I	33	Mx+	0.07	V	NaN	1621	APS	I	22	Mx−	0.06	V	NaN
1572	APS	I	MxP	Mx+	0.07	V	NaN	1622	APS	I	33	Mx−	0.06	V	NaN
1573	APS	I	MnP	Mx+	0.07	V	NaN	1623	APS	I	MxP	Mx−	0.06	V	NaN
1574	APS	I	13	Mx+	0.07	V	NaN	1624	APS	I	MnP	Mx−	0.06	V	NaN
1575	APS	I	23	Mx+	0.07	V	NaN	1625	APS	I	12	Mx−	0.06	V	NaN
1576	APS	I	MxS		0.07	V	NaN	1626	APS	I	13	Mx−	0.06	V	NaN
1577	APS	I	"M"		0.07	V	NaN	1627	APS	I	11	Mx−	0.07	V	NaN
1578	APS	I	11	Mx+	0.08	V	NaN	1628	APS	I	22	Mx−	0.07	V	NaN
1579	APS	I	22	Mx+	0.08	V	NaN	1629	APS	I	33	Mx−	0.07	V	NaN
1580	APS	I	33	Mx+	0.08	V	NaN	1630	APS	I	MxP	Mx−	0.07	V	NaN
1581	APS	I	MxP	Mx+	0.08	V	NaN	1631	APS	I	MnP	Mx−	0.07	V	NaN
1582	APS	I	MnP	Mx+	0.08	V	NaN	1632	APS	I	12	Mx−	0.07	V	NaN
1583	APS	I	12	Mx+	0.08	V	NaN	1633	APS	I	13	Mx−	0.07	V	NaN
1584	APS	I	13	Mx+	0.08	V	NaN	1634	APS	I	11	Mx−	0.08	V	NaN
1585	APS	I	23	Mx+	0.08	V	NaN	1635	APS	I	22	Mx−	0.08	V	NaN
1586	APS	I	MxS		0.08	V	NaN	1636	APS	I	33	Mx−	0.08	V	NaN
1587	APS	I	"M"		0.08	V	NaN	1637	APS	I	MxP	Mx−	0.08	V	NaN
1588	APS	I	11	Mx+	0.09	V	NaN	1638	APS	I	MnP	Mx−	0.08	V	NaN
1589	APS	I	22	Mx+	0.09	V	NaN	1639	APS	I	12	Mx−	0.08	V	NaN
1590	APS	I	33	Mx+	0.09	V	NaN	1640	APS	I	13	Mx−	0.08	V	NaN
1591	APS	I	MxP	Mx+	0.09	V	NaN	1641	APS	I	23	Mx−	0.08	V	NaN
1592	APS	I	MnP	Mx+	0.09	V	NaN	1642	APS	I	11	Mx−	0.09	V	NaN
1593	APS	I	12	Mx+	0.09	V	NaN	1643	APS	I	22	Mx−	0.09	V	NaN
1594	APS	I	13	Mx+	0.09	V	NaN	1644	APS	I	33	Mx−	0.09	V	NaN
1595	APS	I	23	Mx+	0.09	V	NaN	1645	APS	I	MxP	Mx−	0.09	V	NaN
1596	APS	I	MxS		0.09	V	NaN	1646	APS	I	MnP	Mx−	0.09	V	NaN
1597	APS	I	"E"		0.09	V	NaN	1647	APS	I	12	Mx−	0.09	V	NaN
1598	APS	I	"M"		0.09	V	NaN	1648	APS	I	13	Mx−	0.09	V	NaN
1599	APS	I	12	Mx−	0.02	V	NaN	1649	APS	I	23	Mx−	0.09	V	NaN
1600	APS	I	13	Mx−	0.02	V	NaN	1650	APS	I	11	|M|	0.03	V	NaN
1601	APS	I	11	Mx−	0.03	V	NaN	1651	APS	I	22	|M|	0.03	V	NaN
1602	APS	I	22	Mx−	0.03	V	NaN	1652	APS	I	33	|M|	0.03	V	NaN
1603	APS	I	33	Mx−	0.03	V	NaN	1653	APS	I	13	|M|	0.03	V	NaN
1604	APS	I	MxP	Mx−	0.03	V	NaN	1654	APS	I	11	|M|	0.04	V	NaN
1605	APS	I	12	Mx−	0.03	V	NaN	1655	APS	I	22	|M|	0.04	V	NaN
1606	APS	I	13	Mx−	0.03	V	NaN	1656	APS	I	33	|M|	0.04	V	NaN
1607	APS	I	11	Mx−	0.04	V	NaN	1657	APS	I	MxP	|M|	0.04	V	NaN
1608	APS	I	22	Mx−	0.04	V	NaN	1658	APS	I	13	|M|	0.04	V	NaN
1609	APS	I	33	Mx−	0.04	V	NaN	1659	APS	I	11	|M|	0.05	V	NaN
1610	APS	I	MxP	Mx−	0.04	V	NaN	1660	APS	I	22	|M|	0.05	V	NaN
1611	APS	I	12	Mx−	0.04	V	NaN	1661	APS	I	33	|M|	0.05	V	NaN
1612	APS	I	13	Mx−	0.04	V	NaN	1662	APS	I	MxP	|M|	0.05	V	NaN
1613	APS	I	11	Mx−	0.05	V	NaN	1663	APS	I	MnP	|M|	0.05	V	NaN
1614	APS	I	22	Mx−	0.05	V	NaN	1664	APS	I	13	|M|	0.05	V	NaN
1615	APS	I	33	Mx−	0.05	V	NaN	1665	APS	I	11	|M|	0.06	V	NaN
1616	APS	I	MxP	Mx−	0.05	V	NaN	1666	APS	I	22	|M|	0.06	V	NaN
1617	APS	I	MnP	Mx−	0.05	V	NaN	1667	APS	I	33	|M|	0.06	V	NaN
1618	APS	I	12	Mx−	0.05	V	NaN	1668	APS	I	MxP	|M|	0.06	V	NaN
1619	APS	I	13	Mx−	0.05	V	NaN	1669	APS	I	MnP	|M|	0.06	V	NaN
1620	APS	I	11	Mx−	0.06	V	NaN	1670	APS	I	13	|M|	0.06	V	NaN
1671	APS	I	11	|M|	0.07	V	NaN	1721	APS	I	22	Res	0.03	V	NaN
1672	APS	I	22	|M|	0.07	V	NaN	1722	APS	I	33	Res	0.03	V	NaN
1673	APS	I	33	|M|	0.07	V	NaN	1723	APS	I	MxP	Res	0.03	V	NaN

Rank	Stm	TD	Cmp	Rgy	Thrsh	Mtl	Q	Rank	Stm	TD	Cmp	Rgy	Thrsh	Mtl	Q
1674	APS	I	MxP	|M|	0.07	V	NaN	1724	APS	I	MnP	Res	0.03	V	NaN
1675	APS	I	MnP	|M|	0.07	V	NaN	1725	APS	I	12	Res	0.03	V	NaN
1676	APS	I	13	|M|	0.07	V	NaN	1726	APS	I	13	Res	0.03	V	NaN
1677	APS	I	11	|M|	0.08	V	NaN	1727	APS	I	23	Res	0.03	V	NaN
1678	APS	I	22	|M|	0.08	V	NaN	1728	APS	I	MxS	Res	0.03	V	NaN
1679	APS	I	33	|M|	0.08	V	NaN	1729	APS	I	11	Res	0.04	V	NaN
1680	APS	I	MxP	|M|	0.08	V	NaN	1730	APS	I	22	Res	0.04	V	NaN
1681	APS	I	MnP	|M|	0.08	V	NaN	1731	APS	I	33	Res	0.04	V	NaN
1682	APS	I	12	|M|	0.08	V	NaN	1732	APS	I	MxP	Res	0.04	V	NaN
1683	APS	I	13	|M|	0.08	V	NaN	1733	APS	I	MnP	Res	0.04	V	NaN
1684	APS	I	23	|M|	0.08	V	NaN	1734	APS	I	12	Res	0.04	V	NaN
1685	APS	I	11	|M|	0.09	V	NaN	1735	APS	I	13	Res	0.04	V	NaN
1686	APS	I	22	|M|	0.09	V	NaN	1736	APS	I	23	Res	0.04	V	NaN
1687	APS	I	33	|M|	0.09	V	NaN	1737	APS	I	MxS	Res	0.04	V	NaN
1688	APS	I	MxP	|M|	0.09	V	NaN	1738	APS	I	"E"	Res	0.04	V	NaN
1689	APS	I	MnP	|M|	0.09	V	NaN	1739	APS	I	"M"	Res	0.04	V	NaN
1690	APS	I	12	|M|	0.09	V	NaN	1740	APS	I	11	Res	0.05	V	NaN
1691	APS	I	13	|M|	0.09	V	NaN	1741	APS	I	22	Res	0.05	V	NaN
1692	APS	I	23	|M|	0.09	V	NaN	1742	APS	I	33	Res	0.05	V	NaN
1693	APS	I	12	Res	0.0005	V	NaN	1743	APS	I	MxP	Res	0.05	V	NaN
1694	APS	I	13	Res	0.0005	V	NaN	1744	APS	I	MnP	Res	0.05	V	NaN
1695	APS	I	12	Res	0.001	V	NaN	1745	APS	I	12	Res	0.05	V	NaN
1696	APS	I	13	Res	0.001	V	NaN	1746	APS	I	13	Res	0.05	V	NaN
1697	APS	I	12	Res	0.002	V	NaN	1747	APS	I	23	Res	0.05	V	NaN
1698	APS	I	13	Res	0.002	V	NaN	1748	APS	I	MxS	Res	0.05	V	NaN
1699	APS	I	12	Res	0.003	V	NaN	1749	APS	I	"E"	Res	0.05	V	NaN
1700	APS	I	13	Res	0.003	V	NaN	1750	APS	I	"M"	Res	0.05	V	NaN
1701	APS	I	12	Res	0.004	V	NaN	1751	APS	I	11	Res	0.06	V	NaN
1702	APS	I	13	Res	0.004	V	NaN	1752	APS	I	22	Res	0.06	V	NaN
1703	APS	I	12	Res	0.005	V	NaN	1753	APS	I	33	Res	0.06	V	NaN
1704	APS	I	13	Res	0.005	V	NaN	1754	APS	I	MxP	Res	0.06	V	NaN
1705	APS	I	12	Res	0.006	V	NaN	1755	APS	I	MnP	Res	0.06	V	NaN
1706	APS	I	13	Res	0.006	V	NaN	1756	APS	I	12	Res	0.06	V	NaN
1707	APS	I	12	Res	0.007	V	NaN	1757	APS	I	13	Res	0.06	V	NaN
1708	APS	I	13	Res	0.007	V	NaN	1758	APS	I	23	Res	0.06	V	NaN
1709	APS	I	12	Res	0.008	V	NaN	1759	APS	I	MxS	Res	0.06	V	NaN
1710	APS	I	13	Res	0.008	V	NaN	1760	APS	I	"E"	Res	0.06	V	NaN
1711	APS	I	12	Res	0.009	V	NaN	1761	APS	I	"M"	Res	0.06	V	NaN
1712	APS	I	13	Res	0.009	V	NaN	1762	APS	I	11	Res	0.07	V	NaN
1713	APS	I	11	Res	0.01	V	NaN	1763	APS	I	22	Res	0.07	V	NaN
1714	APS	I	12	Res	0.01	V	NaN	1764	APS	I	33	Res	0.07	V	NaN
1715	APS	I	13	Res	0.01	V	NaN	1765	APS	I	MxP	Res	0.07	V	NaN
1716	APS	I	11	Res	0.02	V	NaN	1766	APS	I	MnP	Res	0.07	V	NaN
1717	APS	I	12	Res	0.02	V	NaN	1767	APS	I	12	Res	0.07	V	NaN
1718	APS	I	13	Res	0.02	V	NaN	1768	APS	I	13	Res	0.07	V	NaN
1719	APS	I	23	Res	0.02	V	NaN	1769	APS	I	23	Res	0.07	V	NaN
1720	APS	I	11	Res	0.03	V	NaN	1770	APS	I	MxS	Res	0.07	V	NaN
1771	APS	I	"E"	Res	0.07	V	NaN	1821	APS	I	22	Mx+	0.06	X	NaN
1772	APS	I	"M"	Res	0.07	V	NaN	1822	APS	I	33	Mx+	0.06	X	NaN
1773	APS	I	11	Res	0.08	V	NaN	1823	APS	I	MxP	Mx+	0.06	X	NaN
1774	APS	I	22	Res	0.08	V	NaN	1824	APS	I	MnP	Mx+	0.06	X	NaN
1775	APS	I	33	Res	0.08	V	NaN	1825	APS	I	13	Mx+	0.06	X	NaN
1776	APS	I	MxP	Res	0.08	V	NaN	1826	APS	I	23	Mx+	0.06	X	NaN
1777	APS	I	MnP	Res	0.08	V	NaN	1827	APS	I	MxS		0.06	X	NaN
1778	APS	I	12	Res	0.08	V	NaN	1828	APS	I	"M"		0.06	X	NaN
1779	APS	I	13	Res	0.08	V	NaN	1829	APS	I	11	Mx+	0.07	X	NaN

Rank	Stm	TD	Cmp	Rgy	Thrsh	Mtl	Q	Rank	Stm	TD	Cmp	Rgy	Thrsh	Mtl	Q
1780	APS	I	23	Res	0.08	V	NaN	1830	APS	I	22	Mx+	0.07	X	NaN
1781	APS	I	MxS	Res	0.08	V	NaN	1831	APS	I	33	Mx+	0.07	X	NaN
1782	APS	I	“E”	Res	0.08	V	NaN	1832	APS	I	MxP	Mx+	0.07	X	NaN
1783	APS	I	“M”	Res	0.08	V	NaN	1833	APS	I	MnP	Mx+	0.07	X	NaN
1784	APS	I	11	Res	0.09	V	NaN	1834	APS	I	13	Mx+	0.07	X	NaN
1785	APS	I	22	Res	0.09	V	NaN	1835	APS	I	23	Mx+	0.07	X	NaN
1786	APS	I	33	Res	0.09	V	NaN	1836	APS	I	MxS		0.07	X	NaN
1787	APS	I	MxP	Res	0.09	V	NaN	1837	APS	I	“M”		0.07	X	NaN
1788	APS	I	MnP	Res	0.09	V	NaN	1838	APS	I	11	Mx+	0.08	X	NaN
1789	APS	I	12	Res	0.09	V	NaN	1839	APS	I	22	Mx+	0.08	X	NaN
1790	APS	I	13	Res	0.09	V	NaN	1840	APS	I	33	Mx+	0.08	X	NaN
1791	APS	I	23	Res	0.09	V	NaN	1841	APS	I	MxP	Mx+	0.08	X	NaN
1792	APS	I	MxS	Res	0.09	V	NaN	1842	APS	I	MnP	Mx+	0.08	X	NaN
1793	APS	I	“E”	Res	0.09	V	NaN	1843	APS	I	12	Mx+	0.08	X	NaN
1794	APS	I	“M”	Res	0.09	V	NaN	1844	APS	I	13	Mx+	0.08	X	NaN
1795	PS	H	22	(−)		X	NaN	1845	APS	I	23	Mx+	0.08	X	NaN
1796	PS	H	13	(−)		X	NaN	1846	APS	I	MxS		0.08	X	NaN
1797	APS	I	11	Mx+	0.02	X	NaN	1847	APS	I	“M”		0.08	X	NaN
1798	APS	I	11	Mx+	0.03	X	NaN	1848	APS	I	11	Mx+	0.09	X	NaN
1799	APS	I	22	Mx+	0.03	X	NaN	1849	APS	I	22	Mx+	0.09	X	NaN
1800	APS	I	33	Mx+	0.03	X	NaN	1850	APS	I	33	Mx+	0.09	X	NaN
1801	APS	I	MnP	Mx+	0.03	X	NaN	1851	APS	I	MxP	Mx+	0.09	X	NaN
1802	APS	I	13	Mx+	0.03	X	NaN	1852	APS	I	MnP	Mx+	0.09	X	NaN
1803	APS	I	23	Mx+	0.03	X	NaN	1853	APS	I	12	Mx+	0.09	X	NaN
1804	APS	I	11	Mx+	0.04	X	NaN	1854	APS	I	13	Mx+	0.09	X	NaN
1805	APS	I	22	Mx+	0.04	X	NaN	1855	APS	I	23	Mx+	0.09	X	NaN
1806	APS	I	33	Mx+	0.04	X	NaN	1856	APS	I	MxS		0.09	X	NaN
1807	APS	I	MxP	Mx+	0.04	X	NaN	1857	APS	I	“E”		0.09	X	NaN
1808	APS	I	MnP	Mx+	0.04	X	NaN	1858	APS	I	“M”		0.09	X	NaN
1809	APS	I	13	Mx+	0.04	X	NaN	1859	APS	I	12	Mx−	0.02	X	NaN
1810	APS	I	23	Mx+	0.04	X	NaN	1860	APS	I	13	Mx−	0.02	X	NaN
1811	APS	I	11	Mx+	0.05	X	NaN	1861	APS	I	11	Mx−	0.03	X	NaN
1812	APS	I	22	Mx+	0.05	X	NaN	1862	APS	I	22	Mx−	0.03	X	NaN
1813	APS	I	33	Mx+	0.05	X	NaN	1863	APS	I	33	Mx−	0.03	X	NaN
1814	APS	I	MxP	Mx+	0.05	X	NaN	1864	APS	I	MxP	Mx−	0.03	X	NaN
1815	APS	I	MnP	Mx+	0.05	X	NaN	1865	APS	I	12	Mx−	0.03	X	NaN
1816	APS	I	13	Mx+	0.05	X	NaN	1866	APS	I	13	Mx−	0.03	X	NaN
1817	APS	I	23	Mx+	0.05	X	NaN	1867	APS	I	11	Mx−	0.04	X	NaN
1818	APS	I	MxS		0.05	X	NaN	1868	APS	I	22	Mx−	0.04	X	NaN
1819	APS	I	“M”		0.05	X	NaN	1869	APS	I	33	Mx−	0.04	X	NaN
1820	APS	I	11	Mx+	0.06	X	NaN	1870	APS	I	MxP	Mx−	0.04	X	NaN
1871	APS	I	12	Mx−	0.04	X	NaN	1921	APS	I	33	|M|	0.05	X	NaN
1872	APS	I	13	Mx−	0.04	X	NaN	1922	APS	I	MxP	|M|	0.05	X	NaN
1873	APS	I	11	Mx−	0.05	X	NaN	1923	APS	I	MnP	|M|	0.05	X	NaN
1874	APS	I	22	Mx−	0.05	X	NaN	1924	APS	I	13	|M|	0.05	X	NaN
1875	APS	I	33	Mx−	0.05	X	NaN	1925	APS	I	11	|M|	0.06	X	NaN
1876	APS	I	MxP	Mx−	0.05	X	NaN	1926	APS	I	22	|M|	0.06	X	NaN
1877	APS	I	MnP	Mx−	0.05	X	NaN	1927	APS	I	33	|M|	0.06	X	NaN
1878	APS	I	12	Mx−	0.05	X	NaN	1928	APS	I	MxP	|M|	0.06	X	NaN
1879	APS	I	13	Mx−	0.05	X	NaN	1929	APS	I	MnP	|M|	0.06	X	NaN
1880	APS	I	11	Mx−	0.06	X	NaN	1930	APS	I	13	|M|	0.06	X	NaN
1881	APS	I	22	Mx−	0.06	X	NaN	1931	APS	I	11	|M|	0.07	X	NaN
1882	APS	I	33	Mx−	0.06	X	NaN	1932	APS	I	22	|M|	0.07	X	NaN
1883	APS	I	MxP	Mx−	0.06	X	NaN	1933	APS	I	33	|M|	0.07	X	NaN
1884	APS	I	MnP	Mx−	0.06	X	NaN	1934	APS	I	MxP	|M|	0.07	X	NaN
1885	APS	I	12	Mx−	0.06	X	NaN	1935	APS	I	MnP	|M|	0.07	X	NaN

Rank	Stm	TD	Cmp	Rgy	Thrsh	Mtl	Q	Rank	Stm	TD	Cmp	Rgy	Thrsh	Mtl	Q
1886	APS	I	13	Mx−	0.06	X	NaN	1936	APS	I	13	|M|	0.07	X	NaN
1887	APS	I	11	Mx−	0.07	X	NaN	1937	APS	I	11	|M|	0.08	X	NaN
1888	APS	I	22	Mx−	0.07	X	NaN	1938	APS	I	22	|M|	0.08	X	NaN
1889	APS	I	33	Mx−	0.07	X	NaN	1939	APS	I	33	|M|	0.08	X	NaN
1890	APS	I	MxP	Mx−	0.07	X	NaN	1940	APS	I	MxP	|M|	0.08	X	NaN
1891	APS	I	MnP	Mx−	0.07	X	NaN	1941	APS	I	MnP	|M|	0.08	X	NaN
1892	APS	I	12	Mx−	0.07	X	NaN	1942	APS	I	12	|M|	0.08	X	NaN
1893	APS	I	13	Mx−	0.07	X	NaN	1943	APS	I	13	|M|	0.08	X	NaN
1894	APS	I	11	Mx−	0.08	X	NaN	1944	APS	I	23	|M|	0.08	X	NaN
1895	APS	I	22	Mx−	0.08	X	NaN	1945	APS	I	11	|M|	0.09	X	NaN
1896	APS	I	33	Mx−	0.08	X	NaN	1946	APS	I	22	|M|	0.09	X	NaN
1897	APS	I	MxP	Mx−	0.08	X	NaN	1947	APS	I	33	|M|	0.09	X	NaN
1898	APS	I	MnP	Mx−	0.08	X	NaN	1948	APS	I	MxP	|M|	0.09	X	NaN
1899	APS	I	12	Mx−	0.08	X	NaN	1949	APS	I	MnP	|M|	0.09	X	NaN
1900	APS	I	13	Mx−	0.08	X	NaN	1950	APS	I	12	|M|	0.09	X	NaN
1901	APS	I	23	Mx−	0.08	X	NaN	1951	APS	I	13	|M|	0.09	X	NaN
1902	APS	I	11	Mx−	0.09	X	NaN	1952	APS	I	23	|M|	0.09	X	NaN
1903	APS	I	22	Mx−	0.09	X	NaN	1953	APS	I	12	Res	0.0005	X	NaN
1904	APS	I	33	Mx−	0.09	X	NaN	1954	APS	I	13	Res	0.0005	X	NaN
1905	APS	I	MxP	Mx−	0.09	X	NaN	1955	APS	I	12	Res	0.001	X	NaN
1906	APS	I	MnP	Mx−	0.09	X	NaN	1956	APS	I	13	Res	0.001	X	NaN
1907	APS	I	12	Mx−	0.09	X	NaN	1957	APS	I	12	Res	0.002	X	NaN
1908	APS	I	13	Mx−	0.09	X	NaN	1958	APS	I	13	Res	0.002	X	NaN
1909	APS	I	23	Mx−	0.09	X	NaN	1959	APS	I	12	Res	0.003	X	NaN
1910	APS	I	11	|M|	0.03	X	NaN	1960	APS	I	13	Res	0.003	X	NaN
1911	APS	I	22	|M|	0.03	X	NaN	1961	APS	I	12	Res	0.004	X	NaN
1912	APS	I	33	|M|	0.03	X	NaN	1962	APS	I	13	Res	0.004	X	NaN
1913	APS	I	13	|M|	0.03	X	NaN	1963	APS	I	12	Res	0.005	X	NaN
1914	APS	I	11	|M|	0.04	X	NaN	1964	APS	I	13	Res	0.005	X	NaN
1915	APS	I	22	|M|	0.04	X	NaN	1965	APS	I	12	Res	0.006	X	NaN
1916	APS	I	33	|M|	0.04	X	NaN	1966	APS	I	13	Res	0.006	X	NaN
1917	APS	I	MxP	|M|	0.04	X	NaN	1967	APS	I	12	Res	0.007	X	NaN
1918	APS	I	13	|M|	0.04	X	NaN	1968	APS	I	13	Res	0.007	X	NaN
1919	APS	I	11	|M|	0.05	X	NaN	1969	APS	I	12	Res	0.008	X	NaN
1920	APS	I	22	|M|	0.05	X	NaN	1970	APS	I	13	Res	0.008	X	NaN
Rank	Stm	TD	Cmp	Rgy	Thrsh	Mtl	Q	Rank	Stm	TD	Cmp	Rgy	Thrsh	Mtl	Q
1971	APS	I	12	Res	0.009	X	NaN	2021	APS	I	"M"	Res	0.06	X	NaN
1972	APS	I	13	Res	0.009	X	NaN	2022	APS	I	11	Res	0.07	X	NaN
1973	APS	I	11	Res	0.01	X	NaN	2023	APS	I	22	Res	0.07	X	NaN
1974	APS	I	12	Res	0.01	X	NaN	2024	APS	I	33	Res	0.07	X	NaN
1975	APS	I	13	Res	0.01	X	NaN	2025	APS	I	MxP	Res	0.07	X	NaN
1976	APS	I	11	Res	0.02	X	NaN	2026	APS	I	MnP	Res	0.07	X	NaN
1977	APS	I	12	Res	0.02	X	NaN	2027	APS	I	12	Res	0.07	X	NaN
1978	APS	I	13	Res	0.02	X	NaN	2028	APS	I	13	Res	0.07	X	NaN
1979	APS	I	23	Res	0.02	X	NaN	2029	APS	I	23	Res	0.07	X	NaN
1980	APS	I	11	Res	0.03	X	NaN	2030	APS	I	MxS	Res	0.07	X	NaN
1981	APS	I	22	Res	0.03	X	NaN	2031	APS	I	"E"	Res	0.07	X	NaN
1982	APS	I	33	Res	0.03	X	NaN	2032	APS	I	"M"	Res	0.07	X	NaN
1983	APS	I	MxP	Res	0.03	X	NaN	2033	APS	I	11	Res	0.08	X	NaN
1984	APS	I	MnP	Res	0.03	X	NaN	2034	APS	I	22	Res	0.08	X	NaN
1985	APS	I	12	Res	0.03	X	NaN	2035	APS	I	33	Res	0.08	X	NaN
1986	APS	I	13	Res	0.03	X	NaN	2036	APS	I	MxP	Res	0.08	X	NaN
1987	APS	I	23	Res	0.03	X	NaN	2037	APS	I	MnP	Res	0.08	X	NaN
1988	APS	I	MxS	Res	0.03	X	NaN	2038	APS	I	12	Res	0.08	X	NaN
1989	APS	I	11	Res	0.04	X	NaN	2039	APS	I	13	Res	0.08	X	NaN
1990	APS	I	22	Res	0.04	X	NaN	2040	APS	I	23	Res	0.08	X	NaN

Rank	Stm	TD	Cmp	Rgy	Thrsh	Mtl	Q
1991	APS	I	33	Res	0.04	X	NaN
1992	APS	I	MxP	Res	0.04	X	NaN
1993	APS	I	MnP	Res	0.04	X	NaN
1994	APS	I	12	Res	0.04	X	NaN
1995	APS	I	13	Res	0.04	X	NaN
1996	APS	I	23	Res	0.04	X	NaN
1997	APS	I	MxS	Res	0.04	X	NaN
1998	APS	I	“E”	Res	0.04	X	NaN
1999	APS	I	“M”	Res	0.04	X	NaN
2000	APS	I	11	Res	0.05	X	NaN
2001	APS	I	22	Res	0.05	X	NaN
2002	APS	I	33	Res	0.05	X	NaN
2003	APS	I	MxP	Res	0.05	X	NaN
2004	APS	I	MnP	Res	0.05	X	NaN
2005	APS	I	12	Res	0.05	X	NaN
2006	APS	I	13	Res	0.05	X	NaN
2007	APS	I	23	Res	0.05	X	NaN
2008	APS	I	MxS	Res	0.05	X	NaN
2009	APS	I	“E”	Res	0.05	X	NaN
2010	APS	I	“M”	Res	0.05	X	NaN
2011	APS	I	11	Res	0.06	X	NaN
2012	APS	I	22	Res	0.06	X	NaN
2013	APS	I	33	Res	0.06	X	NaN
2014	APS	I	MxP	Res	0.06	X	NaN
2015	APS	I	MnP	Res	0.06	X	NaN
2016	APS	I	12	Res	0.06	X	NaN
2017	APS	I	13	Res	0.06	X	NaN
2018	APS	I	23	Res	0.06	X	NaN
2019	APS	I	MxS	Res	0.06	X	NaN
2020	APS	I	“E”	Res	0.06	X	NaN
2041	APS	I	MxS	Res	0.08	X	NaN
2042	APS	I	“E”	Res	0.08	X	NaN
2043	APS	I	“M”	Res	0.08	X	NaN
2044	APS	I	11	Res	0.09	X	NaN
2045	APS	I	22	Res	0.09	X	NaN
2046	APS	I	33	Res	0.09	X	NaN
2047	APS	I	MxP	Res	0.09	X	NaN
2048	APS	I	MnP	Res	0.09	X	NaN
2049	APS	I	12	Res	0.09	X	NaN
2050	APS	I	13	Res	0.09	X	NaN
2051	APS	I	23	Res	0.09	X	NaN
2052	APS	I	MxS	Res	0.09	X	NaN
2053	APS	I	“E”	Res	0.09	X	NaN
2054	APS	I	“M”	Res	0.09	X	NaN